UNIVERSITY OF CAPE TOWN

DEPARTMENT OF CIVIL ENGINEERING

RESEARCH PROJECT

CIV 4044S

RESEARCH TOPIC

Modelling of Residual Stresses of Blood Vessels

Author:

Mr. Emmanuel Omatuku Ngongo

Supervisor:

Dr Sebastian Skatulla

In partial fulfilment of the requirements for the degree of Bachelor of Science in Civil Engineering

23 November 2015

Plagiarism declaration

i) I know that plagiarism is wrong. Plagiarism is to use another's work and pretend that it is one's own.

ii) I have used the Harvard convention for citation and referencing. Each contribution to, and quotation in, this research from the work(s) of other people has been attributed, and has been cited and referenced.

iii) This research is my own work.

iv) I have not allowed, and will not allow, anyone to copy my work with the intention of passing it off as his or her own work.

v) I acknowledge that copying someone else's work, or part of it, is wrong, and declare that this is my own work.

Signature: 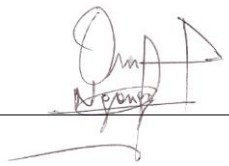

Abstract

The diagnosis of vascular diseases can be achieved with a suitably determined circumferential stress at arterial walls. The stress distribution over arterial walls in blood vessels is affected by residual stresses and stresses due to blood pressure. However, residual stresses are still not reliably determined. For this reason, a suitable incorporation of these stresses is required in order to establish the wall stress as a reliable diagnostic indicator. Thus this study aims to model residual stresses by incorporating them into the wall stress distribution, and to investigate the effect that parameters defining the study constitutive model have on the stress distribution.

The constitutive model makes use of the *Cosserat* fibre continuum in order to account for mechanics of arterial walls. It was developed for cardiac tissues by Skatulla et al. (2014), but it can also be used for a preliminary investigation on arterial tissues as these two types of tissues exhibit comparable mechanics.

Residual stresses are incorporated by using three problem definitions, which are derived from the opening angle method, into a three dimensional two-layer artery consisting of the media and adventitia. The first problem incorporates residual stresses that are locked within individual load-free layers. The second problem continues the first problem by incorporating residual stresses acting at the interface surface between arterial layers, and then determine the artery wall stress distribution under blood pressure. The third problem determines the wall stress in the stress-free artery under blood pressure. On the other hand, the effect of parameters defining the constitutive model is investigated by varying the size of parameters in these problems.

However, the second problem is not analysed in this study because it requires an analysis implementation that could not be achieved within the study timeline. Similarly, model parameters of problems are not calibrated to available experimental data. Therefore, this study only provides qualitative results.

The investigation results on the incorporation of residual stresses into the stress distribution are found to be inconclusive as they provide contradictory results. The characteristic scaling parameters are found to influence the magnitude and gradient of the stress distribution. However, these results are not conclusive to clearly define the influence. Thus it is recommended that further research be conducted in order to gain conclusive results.

Acknowledgements

Firstly, I would like to thank my research supervisor, Dr Sebastian Skatulla, for providing me with such an interesting topic to undertake. Without his assistance and dedicated involvement in every step throughout the process, this document would have never been accomplished. Moreover, Dr Skatulla has shown a high level of patience and enthusiasm while explaining countless topics, and I would also like to show my gratitude for that.

Secondly, I would like to thank my whole family for their love and support throughout my life as none of this could have happened without them.

Thirdly I would like to thank Tanja Strassberger and Jojo Farida Kyababa for their supports, and my friends who gave me the right diversion from this work and different perspectives.

This study has been supported by the Centre for High Performance Computing in Mowbray, Cape Town.

Table of contents

List of figures

Page

List of tables

Page

1. Introduction

1.1 Background to study

Today it is possible to best reconstruct patient-specific geometries with the help of medical imaging. In the future numerical simulations could be employed to better understand mechanically influenced processes for the purpose of improving medical treatment and assessing the risk potential of degenerated areas. This would require advanced models with the capability to consider multiple biological phenomena, in particular residual stresses. These stresses arise in arterial walls and have an effect on the wall stress.

Several investigations have found that vascular diseases can be diagnosed with a suitably determined circumferential stress at arterial walls. With this finding, the wall stress could be established as a diagnostic indicator of vascular diseases. On this subject, Cheng et al. (1993) and Li et al. (2006) reported that the application of a suitable stress criteria could gauge the risk potential of plaque rupture, which is supposedly initiated by stress concentration within the arterial wall. However, the establishment of the wall as a diagnostic indicator would require a reliable and precise description of transmural stresses. In this regard, Ohayon et al. (2007) found that residual stresses are over-estimated in the fibrous cap when residual stresses are neglected. Therefore, the incorporation of residual stresses might contribute to a better understanding of possible stress driven growth and remodelling processes, as reported by Greenwald et al. (1997).

1.2 Research motivation, aims and objectives

1.2.1 Motivation for research

Over the last two decades, the mortality rate of vascular diseases has significantly increased. This led to the importance of optimising treatment techniques, which in turn has given rise to the mechanical simulation of arterial walls. At this stage the mechanical simulation of arterial walls is still a developing field. Thus there is a still a need for more contribution into this field so that arterial walls can be simulated as closely as possible to the real arteries in order to best incorporate circumferential residual stresses.

1.2.2 Importance of modelling residual stresses on blood vessels

Several material models have been developed to describe the behaviour of arterial walls. However, most of them present some form of limitation in their applications. In order to incorporate circumferential residual stresses, a material model that has little to no limitation is required. Thus it is of importance that adequate models be developed for the incorporation of residual stresses. This in turn would enable to suitably determine circumferential stresses at arterial walls, and could result in the wall stress being used as a reliable diagnostic indicator for vascular diseases.

1.2.3 Aim of research

This study aims at incorporating circumferential residual stresses into the arterial wall stress distribution under the blood pressure regime. Furthermore, it aims to make use of a constitutive model based on the *Cosserat* fibre continuum. Finally, it aims to investigate the effect of characteristic scaling parameters, which define the constitutive model, on the wall stress distribution.

1.2.4 Objectives of study

The objectives of this study are:

i) Familiarisation with the in-house structural analysis software SESKA;

ii) Presentation of background knowledge required for the analysis of arterial walls in blood vessels and wall stress distribution;

iii) Creation of artery models using the commercial pre-processing software GiD;

iv) Computational analysis of models using the *Cosserat* fibre constitutive law implemented within SESKA by Dr Skatulla;

v) Post-processing of results using GiD in order to gain qualitative results with respect to the wall stress distribution incorporating residual stresses;

vi) Post-processing of results using GiD in order to determine the effect of characteristic scaling parameters of the constitutive model over the stress distribution on arterial walls.

1.3 Scope and limitations of investigation

This study does not attempt to conduct a full analysis of the stress distribution of arterial walls, but rather to gain a preliminary understanding of the incorporation of circumferential residual stresses into the wall stress. In this regard, only qualitative results and discussions are provided. Also included within the scope of this study is the investigation of the constitutive law through the effect of its characteristic scaling parameters on the wall stress distribution.

Moreover, the study analysis is conducted using a constitutive model based on the *Cosserat* fibre continuum. The model is implemented within the existing computational continuum mechanics framework which is contained in SESKA. With regard to the pre- and post- processing of models, the commercial software package GiD is used.

1.4 Layout of this document

This study is structured as follows. In **Chapter 2**, residual stresses of arterial walls are discussed with focus on the definition, origin and effect over the wall stress distribution. A review of the mechanics of arterial walls is then provided with respect to the structure composition and mechanical properties of arterial layers. This is followed by an outline of one of the procedures that are used to identify material parameters of arterial layers in experiments and computational models. Subsequently, a method of investigation into the incorporation of circumferential residual stresses is reported. Finally, concluding remarks over the reviewed literature are provided at the end of the chapter.

The continuum mechanical framework used in this work is explained in **Chapter 3.** A short review of the constitutive model, which is based on the *Cosserat* fibre continuum, is given. Thereafter, the study principles of computer analysis are introduced in **Chapter 4**. Within this chapter, a short introduction into the variational formulation is also provided as well as a description of the assembly of system of equations.

Numerical examples based on the literature review and outlined continuum mechanics theory are developed in **Chapter 5**. Here the problem definitions for the incorporation of circumferential residual stresses are explained. Thereafter, simulations of characteristic scaling parameters defining the constitutive model are presented, and their results discussed.

Chapter 6 provides conclusions and recommendations of the investigation.

2. Literature review

2.1 Introduction

In this chapter, the available literature on circumferential residual stresses and the material of arterial walls of blood vessels are reviewed. Initially, an introduction to circumferential residual stresses in arterial walls is developed with the intention to familiarise the reader with the research topic. This is followed by the description of the mechanics of arterial walls. Subsequently, the process used to identify material parameters of arterial walls in experiments and computation models is presented. Finally, previously conducted investigations are reviewed with the attention being given to the method of investigation into the modelling and incorporation of circumferential residual stresses acting in arterial walls.

2.2 Residual stresses in arterial walls blood vessels

Residual stresses refer to self-equilibrating stresses that are locked into a material in the absence or presence of any external loads. They result from any mechanical process which can cause deformation. The state of residual stresses depends on both the prior processes that a material has undergone, and the mechanical properties that relate the current mechanical environment to deformation (Cheng and Finnie, 2007).

Until the early 1980's arterial walls of load-free blood vessels were assumed to be stress free. This assumption was disproved experimentally by Vaishnav and Vossoughi (1983). During their experiment, they observed that the radial cut of circular rings of bovine and porcine abdominal arteries causes rings to open up into a horseshoe configuration; see Figure 2-1 for a schematic representation. Consequently, this led to the conclusion that an artery, which is intact and load-free, is under the action of residual stresses in the circumferential direction. However, it seems that Bergel (1960) was the first to observe this phenomenon (Schröder and Brinkhues, 2014).

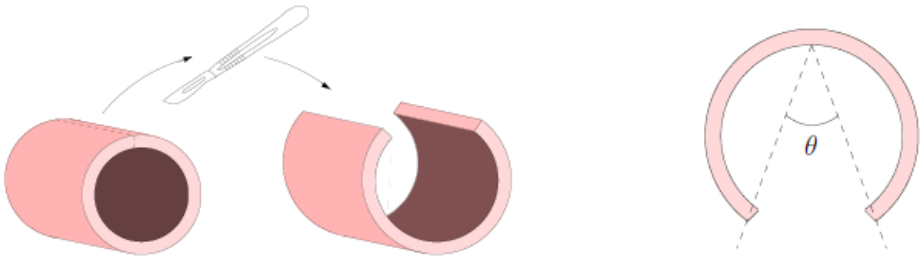

Figure 2-1: Schematic of radial cut through an artery and resulting opening angle (Brinkhues, 2012)

With the presence of circumferential residual stresses in arterial walls proven, several investigations into their origin and properties were conducted. On this subject, Cardamone et al. (2009) established that residual stresses originate from the non-uniform growth and remodelling process, which result in incompatibility. This was corroborated with observations that residual stresses increase during life. In this regard, Fung and Liu (1989) reported that an increase or a decrease in blood pressure over a short period of days influences significantly residual stresses. Furthermore, it was found that the distribution of residual stresses can also be altered as a result of hypertrophy that may cause further growth of adult in-vivo arteries. Additionally, it was found that there are other circumstances that influence residual stresses. About this influence, Zeller and Skalak (1998) showed that the muscle tone impacts changes in residual stresses. It was also found that osmotic interactions on the micro-level induce residual stresses. These are interactions between tissue layers and between the tissue and blood (Schröder and Brinkhues, 2014).

Circumferential residual stresses are found to be compressive in the inner wall and tensile in the outer wall of a load-free artery (Pierre et al., 2012). As a consequence, they have a significant effect on the stress gradient of the artery. In fact, Chuong and Fung (1986) and Fung (1991) found that residual stresses cause a significant reduction in the magnitude of stresses and stress gradient of an artery under blood pressure. With respect to the wall strain distribution, Takamizawa and Hayashi (1987) developed the uniform strain hypothesis. The latter states that residual stresses cause an almost uniform circumferential strain distribution under blood pressure. Furthermore, experimental observations of Nollert et al. (1992) showed that the reduction in the stress gradient at the inner side of the arterial wall may reduce the risk of atherogenesis, which is the formation of abnormal fatty or lipid masses in arterial walls.

2.3 Mechanics of arterial walls of blood vessels

2.3.1 Structure of arterial walls

Arterial walls of blood vessels can be divided in three distinct cylindrical sections as illustrated in Figure 2-2. These sections have distinct structural functions in terms of the blood vessel physiology and mechanical properties. They are the intima, the media and the adventitia (Canfield and Dobrin, 2007).

The intima is the innermost layer. It comprises primarily a thin monolayer of endothelial cells lining the arterial wall, a thin basal membrane and a subendothelial layer. The endothelial cells have little influence on the mechanics of blood vessels, but play an important role in hemodynamics and transport phenomena. As a consequence to their anatomic location, they are subjected to large variations in stress and strain. The variations are due to pulsatile changes in blood pressure and flow (Canfield and Dobrin, 2007). The subendothelial layer consists mainly of thinly dispersed smooth muscle cells and bundles of collagen fibrils (Gasser et al., 2006).

The media is the middle layer and represents the major portion of the arterial wall. It provides most of the mechanical strength necessary to sustain the structural integrity of the wall. In its composition, it consists of a complex three-dimensional network of smooth muscle cells, elastin and bundles of collagen fibrils (Clark and Glagov, 1979). The collagen fibres are found within bands of smooth muscle and may participate in the transfer of forces between the smooth muscle cells and elastic lamellae. The elastic lamellae are composed principally of the fibrous protein elastin. The number of elastic lamellae depends on the wall thickness and the anatomical location (Wolinsky and Glagov, 1969). In the case of the canine carotid, the elastic lamellae account for a major component of the static structural response of the blood vessel (Dobrin and Canfield, 1984). This response is modulated by the smooth muscle cells, which have the ability to actively change the mechanical characteristics of the arterial wall (Dobrin and Rovick, 1969).

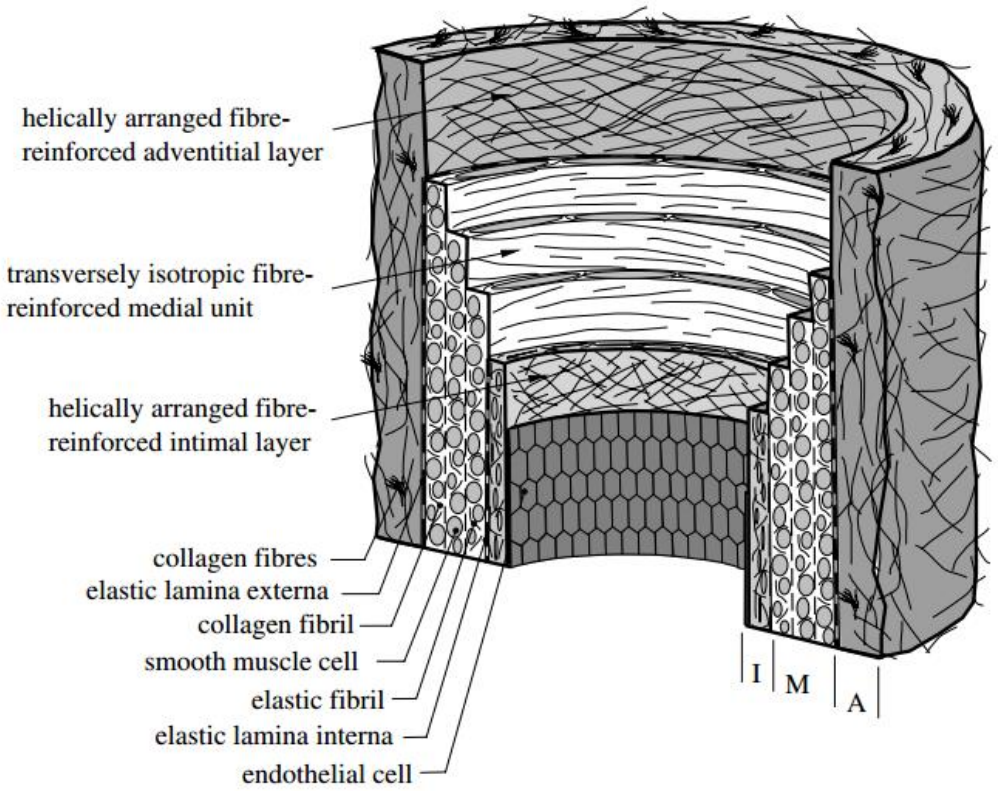

Figure 2-2: Histomechanical idealisation of a healthy artery (Gasser et al., 2006)

The adventitia is the outermost layer surrounded by loose and disorganized fibrous connective tissue, which may have less influence on the mechanics of blood vessels. The primary constituents of the adventitia are thick bundles of collagen fibrils arranged in helical structures. The thickness of the adventitia depends strongly on the physiological function of the blood vessel and its topographical site (Canfield and Dobrin, 2007).

2.3.2 Mechanical properties of arterial walls

The understanding of the mechanical response of arterial walls is essential for the development of a reliable constitutive model. In this regard, this section describes the mechanical characteristics of arterial walls that have been proven through several investigations, some dating as far back as a century ago with Roy (1880-1882).

2.3.2.1 Basic arterial properties

The general mechanical characteristics of arterial walls remain the same along the arterial tree, albeit that there are significant variations in mechanical properties of arteries in accordance with histology. The material wall and its layers are anisotropic in virtue of the highly organised structural arrangement (Gasser et al., 2006). In this regard, the non-collagenous matrix exhibits an isotropic behaviour, while collagen fibres exhibit an anisotropic behaviour (Holzapfel et al., 2000)

The artery has the property of a solid-fluid mixture and can be mechanically classified as a 'mixture composite'. The solid part comprises primarily a composite of elastin, collagen and smooth muscle cells (Humphrey, 2002). Because the stress-induced movement of fluid in and out of the wall is generally neglected for many problems of interest, the arterial wall can be, and is most commonly, assumed to be a homogenised solid. This assumption is sufficiently accurate for most experimental and theoretical studies of the wall stress distribution (Gasser et al., 2006). Under these conditions, arteries behave as nearly incompressible solids at physiological loads, as reported by Carew et al. (1968) and Chuong and Fung (1984). Moreover, healthy arteries are composite structures which are highly deformable (Roy, 1880-82) and exhibit a nonlinear stress-strain response (Abè et al., 1996).

2.3.2.2 Stress-free and load-free configurations

The mechanical environment of the arterial wall is generally changing due to several factors such as growth, atrophy, remodelling, repair, ageing, disease, etc. The arterial wall continually adapts to its mechanical environment, and thus undergoes several irreversible processes. Because all these processes take place in the spatial configuration of the arterial wall, the existence of a compatible stress-free (reference) configuration is unlikely (Gasser et al., 2006). As a consequence, the load-free configuration of an artery is residually stressed, as firstly reported by Vaishnav and Vossoughi (1983).

The cut of an intact load-free arterial ring causes the ring to respond by opening up in a horseshoe shape. The opening aims at minimising the stored strain energy and releasing circumferential residual stresses (Gasser et al., 2006). These stresses are different for individual arterial layers (intima, media and adventitia) in the load-free configuration (Greenwald et al., 1997). With regard to the reliable prediction of the stress

state in the loaded arterial wall, it is of crucial importance to first identify the circumferential residual stresses in an intact load-free arterial ring ((Chuong and Fung, 1983) ; (Holzapfel et al., 2000)).

2.4 Parameter identification of arterial layers

This sections outlines one of the procedures that was used to identify material parameters of arterial layers in the literature. Herein a short description of the procedure is provided for an experimental and a computational investigations.

For the experimental data, a specimen was obtained from a human aorta of a 40 years old male. The arterial wall of the specimen was separated into the three arterial layers, i.e., intima, media and adventitia. Then tissue samples were cut out in the circumferential and axial directions in order to obtain two specimens. Subsequently they were preconditioned and underwent uniaxial tension tests. The results of the experimental data of the media and adventitia can be found in Holzapfel et al. (2004) and Holzapfel and Gasser (2007), respectively. Because the intima has little influence on the mechanics of blood vessels, it was not considered for parameter identification.

In Schröder and Brinkhues (2014), model parameters for the experimental data were developed based on the mechanics of arterial layers. They accounted for the anisotropic behaviour of the media and adventitia by making use of an additive composition and energy function, and the incompressible behaviour by making use of the Lagrangian method. Thereafter, they treated the artery as a fibre-reinforced material with fibres corresponding to the collagenous component embedded in the non-collagenous matrix material. The embedded families of fibres were assumed to account for the anisotropic response. In this elastic model, material parameters described the isotropic mechanical response of the non-collagenous matrix, while two specified parameters were associated to the anisotropic response of collagen fibres. Additionally, these parameters include the angle between the two fibre directions and circumferential direction.

2.5 Method of investigation

This section expands on factors influencing the size of the opening angle resulting from the radial cut of a load-free artery. Moreover, it provides an overview of various methods developed for the computation of circumferential residual stresses in an artery. Afterwards, the computational method that is used within this study is presented.

2.5.1 The opening angle

Various investigations have focused on understanding factors that affect the size of the opening angle obtained after the radial cut of an artery; see Figure 2-1 above for the illustration of an opening angle. In this regard, Huang and Yen (1998) found that the angle tends to increase with the general size of the artery. Additionally, the artery was found to continue to open up to 20 minutes after an excised segment was radially cut in Han and Fung (1991). In the investigation of Azeloglu et al. (2008), it is reported how inhomogeneous proteoglycan distributions over the vessel wall influence the opening angle. It was found that the size of the angle increases with increasing osmotic swelling pressure caused by lower salt concentrations of the bathing environment. Furthermore, the opening angle is subject to wide fluctuations along the vascular tree (Fung and Liu, 1989). However, it was found to be independent of the temperature in Han and Fung (1991).

The change in the size of the opening angle is also linked to hypertension and hypertrophy. In this regard, Liu and Fung (1989) found that a change in blood pressure influences residual strains, which consequently causes a significant change in the opening angle. Moreover, the investigation of Vossoughi et al. (1993) on bovine aortas revealed that sliced configurations are not fully stress free and that additional circumferential cuts cause different opening angles for individual arterial layers. This led them to conclude that the size of the opening angle increases in inner layers and decrease in outer layers. This conclusion indicates that some residual stresses still remain after the radial cut of an artery. This was confirmed by the investigations of Schulze-Bauer et al. (2002) on human aortas and Matsumoto et al. (2004) on porcine thoracic aortas.

Moreover, the investigation on rat aortas by Greenwald et al. (1997) resulted in similar conclusions concerning the different sizes of opening angle for individual arterial

layers. Additionally, they revealed that elastase-treated (elimination of elastin) specimens offer smaller opening angles, while collagenase-treated (elimination of collagen) and frozen (destruction of smooth muscle cells) specimens behave like the untreated control specimens. On the other hand, Saini et al. (1995) conducted the first studies on human thoracic and abdominal aortas. They discussed the effect of age, sex, the position along the artery and atherosclerosis on the opening of sliced arterial rings. They found that the value of the opening angle increases with increasing distance from the heart (female: 150°- 200°, male: 200°-250°). Additionally, they also observed larger opening angles in aged and atherosclerotic diseased vessels and in those obtained from male samples.

2.5.2 Scheme for the incorporation of residual stresses

Several methods have been developed over the years in order to incorporate circumferential residual stresses. One of the methods is the use of constitutive models. The latter are extensively used in the computation of residual stresses today, but it was Chuong and Fung (1986) who seem to be the first to use a constitutive model to compute residual stresses. The model described the geometry of an open artery, whose closed initial configuration was regarded as a thick-walled cylindrical tube with constant thickness. To compute residual stresses they used a method which is referred to as the *opening-angle method*. Therewith they computed circumferential residual stresses acting in a two-dimensional load-free and closed artery, and they reported that residual stresses enforce compression on the inner side and tension on the outer side of the arterial wall.

Many publications similarly use the opening angle to achieve an analytical solution for residual strains of initially open ideal tubes, which are closed by an initial bending (Schröder and Brinkhues, 2014). A mathematical model was derived by Rachev (1997) for the stress-dependent remodelling of a two-layer arterial tube. This model catered for the assumption that stress and strain values are equal under hypertensive and normotensive conditions by remodelling the zero-stress configuration through the thickening of layers. In this model, it was observed that residual stresses are present in the opened-up configuration of a hypertensive artery. By way of a one-layer model, Chaudhry et al. (1997) showed that there is a significant reduction of the circumferential stress and stress gradient at the inner wall. Moreover, the opening angle method was applied to a two-

layer tube and different material models were investigated in Holzapfel et al. (2002a). The objectives of this work were to analyse the initial deformation tensor for multi-layered tubes and the effect of residual stresses over the overall stress distribution in the physiological regime.

In Holzapfel and Gasser (2007), the high-pressure response is investigated. The opening-angle method was also applied to more realistic arterial geometries by Pena et al. (2006) who conducted corresponding finite-element simulations. Alastrué et al. (2007) used the opening angle method with a special form of the multiplicative decomposition of the deformation gradient to account for residual stresses. This approach was further investigated with the inclusion of growth in Alastrué et al. (2008) and the implementation in a micro-sphere model in Alastrué et al. (2009). Similarly, Menzel (2007) dealt with growth-induced residual stresses. Cardamone et al. (2009) combined the opening-angle method and a constrained mixture mode of vascular growth and remodelling, where the mixture components were the individual constituents of the artery, i.e. elastin, collagen and smooth muscle. One of the aims of the aforementioned investigations was to find the origin of residual stresses. For the modelling of growth and remodelling in the framework of constrained mixture, see Alford et al. (2008) and Valentin and Humphrey (2009).

The different behaviour of the three arterial layers with different opening angles for each layer was investigated by Holzapfel and Ogden (2010). They provided an extension to the opening-angle method by accounting for bending and stretching in both the circumferential and axial directions with the aim of reflecting the three-dimensional residual stretch and stress state. This modelled was further extended by Bustamante and Holzapfel who accounted for the difference of opening angles along the tube owing to the axial and radial position.

In Stahlhand et al. (2004), the residual-strain state was derived using experimental data. This was achieved by deriving a minimisation problem to provide an approximate identification of material parameters including residual strains. The parameters for residual strains were assumed using the opening angle method. On the other hand, Olsson et al. (2006) used this parameter identification algorithm to determine an initial local deformation tensor, which is able to describe the residual strain. This model was extended by introducing the evolution of growth in Olsson and Klarbring (2008). In Chen

and Eberth (2012), a special class of constitutive functions was introduced without incorporating residual stresses in order to obtain uniform circumferential stresses.

Contrary to the methods mentioned above, a numerical method was used by Balzani et al. (2006). They closed an open artery by means of a displacement-driven finite-element procedure in order to establish a residual strain state. Famaey et al. (2013) also used this procedure to account for a residual stress distribution in the circumferential direction. Additionally, they used longitudinal stretching to apply longitudinal residual stresses. This numerical method is adequate when the geometry of the opened artery is known, but it is numerically extensive.

In Polzer et al (2013), a different method using the isotropic volumetric growth concept is proposed in order to reflect residual stresses. This method minimises stress gradients by applying a certain amount of growth. In contrast, Schröder and Brinkhues (2014) and Schröder and Hoegen (2015) developed a novel method for the incorporation of residual stresses in patient specific three-dimensional arterial models. This method does not use the opening angle as the starting point, but focuses directly on the current stress state within the arterial wall.

In this study, the method that is used for the incorporation of residual stresses is the opening angle method developed by Holzapfel and Gasser (2006). It is a three-dimensional method that consists of a two-step loading procedure. Here a two-layer artery consisting of the media and adventitia is considered. The first step involves the simulation of a load-free and stress-free configuration of the open artery. The second step concerns the simulation of the physiologically loaded and residually stressed configuration of the closd artery. The two steps are briefly discribed below.

Step 1: Load-free and stress-free artery

This step starts with the consideration of individual open configurations of the media and aventitia, as illustrated in Figure 2-3. These configurations are regarded as load-free and stress-free. In order to determine residual stresses acting within the two arterial layers, an initial and pure bending deformation is applied to the open layers at the open surfaces. The deformation is achieved through a displacement driven simulation and results in two closed configurations of arterial layers. The closed configurations are still load-free but residually stressed. Because the residual stresses obtained from the closure

do not account for residual stresses acting at the interface surface between arterial layers, nodes at the interface surface are linked together. This results in one closed two-layer artery, which is residually stressed and has a homogeneous stress and strain states in both the circumferential and radial directions. This state is then used as the reference configuration for the next step.

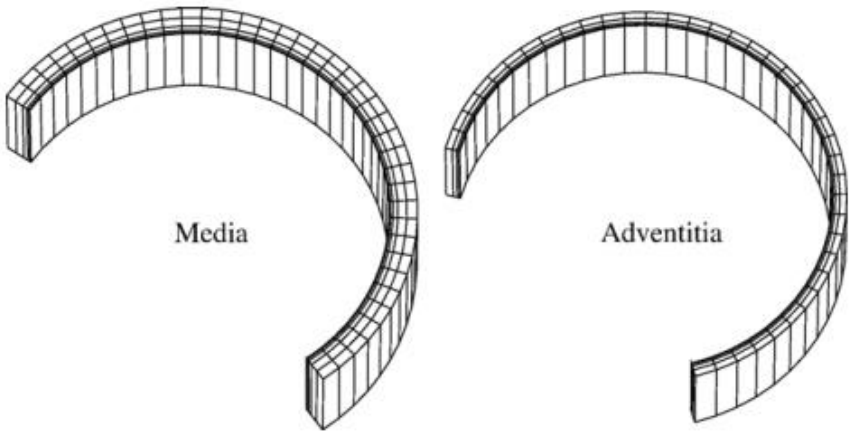

Figure 2-3: Finite element mesh of two independent reference configurations of the media and the adventitia (Holzapfel and Gasser, 2006)

Step 2: Physiological loading

In this step, the two-layer artery obtained in the first step is physiologically loaded with blood pressure. At the end of this step, a circumferential stress distribution through the deformed wall is obtained. Figure 2-4 illustrates the stress distribution obtained from the application of a blood pressure of 13.33 kPa, which assumed to be the mean arterial pressure. This illustration shows that circumferential residual stresses reduce the wall stress gradient and cause an almost uniform stress distribution when they are incorporated in the stress distribution. Moreover, the stress is greater in the media than in the adventitia.

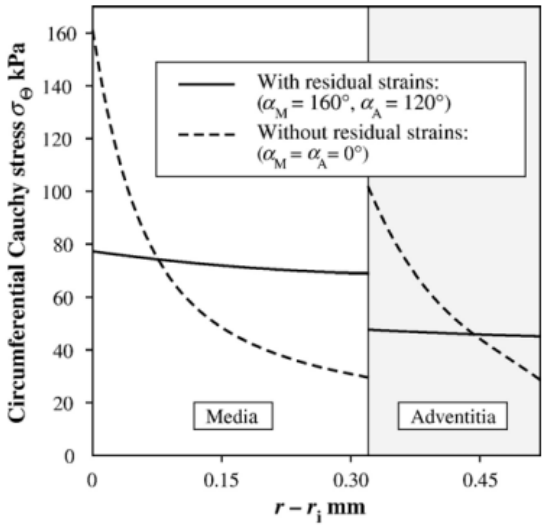

Figure 2-4: Circumferential stress distribution through the deformed wall thickness of the media and adventitia (Holzapfel and Gasser, 2006)

2.6 Concluding remarks

Through the literature review, it was reported that a load-free artery is residually stressed and that circumferential residual stresses are compressive at the inner wall and tensile at the outer wall of arterial layers. It was also reported that residual stresses cause an almost uniform circumferential strain distribution under blood pressure, as stated in the uniform strain hypothesis. Furthermore, it was found that the opening angle varies and is different for individual arterial layers as it tends to increase in inner layers and decrease in outer layers.

Arterial walls consist of three layers, i.e. the intima, media and adventitia, but the intima has little influence on the mechanics of arterials walls. Moreover, arterial tissues mainly consist of an isotropic non-collagenous matrix and anisotropic collagen fibres that provide most of the stiffness. Furthermore, the material of arterial walls can be regarded as an incompressible solid. Additionally, the procedure used to define material parameters was provided in this section.

Several methods of incorporation of residual stresses were briefly mentioned, but it is the opening angle method of Holzapfel and Gasser (2007) that was clearly described in order to be used within this study. It is a three dimensional method making use of a two-layer artery consisting of the media and adventitia.

3. Continuum mechanics theory

3.1 Introduction

Continuum mechanics is a mathematical discipline that deals with the analysis of the mechanical behaviour and kinematics of materials modelled as continuous mass rather than discrete particles. It is concerned with the analysis of bodies that are made up of elements of matter which behave identically to their bodies. Additionally, it analyses such bodies making use of discretisation techniques, tools of algebra, and tools of calculus of vectors and tensors.

The fundamental assumption of continuum mechanics is that the material is continuous and completely fills the space it occupies. The validity of the assumption resides on the fact that engineering analysis commonly deals with bodies which are far larger than the matter from which the body is composed. This implies that if the body is analysed as a whole, or an element within the body is analysed under identical loading and boundary conditions, both analyses will yield identical results. This valid as it is assumed that the underlying molecular structure of the material analysed is generalised by the overlying material properties.

This section begins with a general description of the balance laws of continuum mechanics. Subsequently, this study constitutive model is briefly discussed.

3.2 Balance laws of continuum mechanics

A general description of the laws underlying the method to model finite strain behaviour is required. When subjected to any form of loading (such as force or temperature), the behaviour of a body may be described by the following laws fundamental to continuum mechanics (Mase, 1999):

i) **The law of conservation of mass** ensures that no mass is lost or gained when the body changes from the undeformed to the deformed configuration;

ii) **The law of linear and angular momentum conservation** is related to Newton's second law which defines the rate of change of linear and angular momentum over time, resulting in force and momentum; and

iii) **The law of energy conservation** is related to the principle law of energy which states that energy can neither be created nor destroyed but can only change forms. In this regard, the study constitutive model focuses on the strain energy.

3.3 The constitutive model

The constitutive model of a material aims to reflect the basic mechanical properties that result from the material internal constitution. This study constitutive model is based on the *Cosserat* fibre continuum and was developed by Skatulla et al. (2014) for cardiac tissues. Because cardiac and arterial tissues exhibit comparable mechanical behaviour, this model can be used for preliminary studies on arterial walls. In this section, the *Cosserat* fibre continuum approach is briefly discussed.

3.3.1 *Cosserat* fibre continuum approach

Cardiac tissues, like arterial tissues, can be described as the sum of a combination of myocytes and an extracellular matrix (ECM). The ECM plays a significant role in the mechanics of these tissues as reported by Fomovsky et al. (2010). It has various components, most notably collagen which are responsible for the structural support and contributes to the mechanical stiffness of the problem. Other components include elastin, fibroblasts, plasma cells, endothelial cells and smooth muscle cells. For the development of this constitutive model, Skatulla et al. (2014) considered the components of cardiac tissues under two main categories as depicted in Figure 3-1:

i) The fibrous structure: composed of a bundle of myocytes bound by collagen fibres, which are anisotropic;

ii) The complementary connective tissue: made up from remaining components of the ECM, which are considered isotropic.

This constitutive model describes the characteristics of myocardium by using one-dimensional *Cosserat* continua. This allows for the inclusion of fibre motion relative to the matrix representing the non-local material response due to twisting and bending of a fibre bundle. Thus characteristic scaling parameters associated with the micro-structure become material parameters of the formulation. In this study, the characteristic scaling parameters are represented by parameters c_1 and c_4 that are linked by the relation $c_1 = 2c_4$. Moreover, the constitutive law of this model presents a natural advantage over classical formulations as it can explicitly account for torsion and bending.

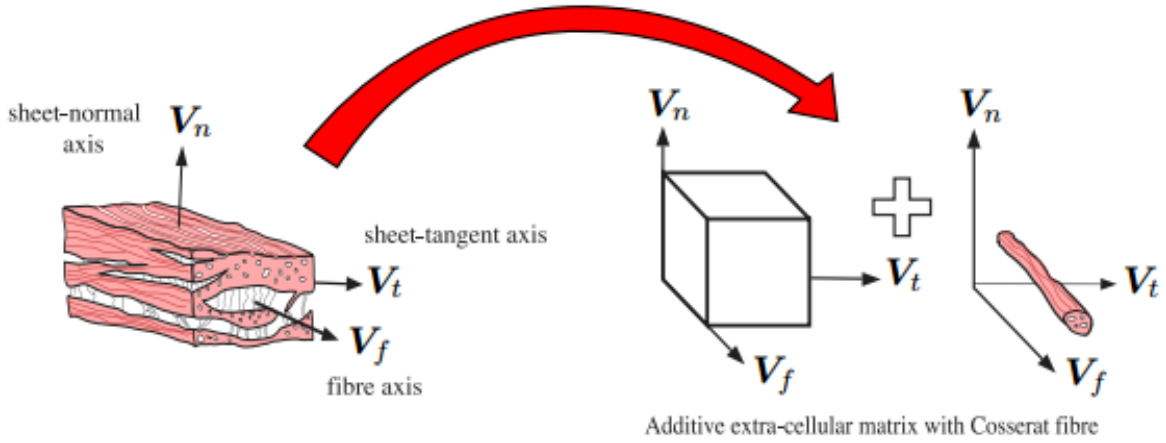

Figure 3-1: Contribution of the three dimensional ECM and fibre bundle (Sack, 2014)

It is quite established in the literature review that myocardial tissues, like arterial tissues, exhibit highly nonlinear properties as a result of the complex fibre-collagen arrangement and composition inherent to the material. Additionally, a hyperplastic material behaviour is assumed for this type of tissues. To account for this material behaviour, this model makes use of a nonlinear strain energy function which includes contributions linked to the *Cosserat*-fibre continuum and complementary terms referring to the ECM.

In this model, the strain energy is decomposed in accordance with the contributions of the fibrous structural components and complementary connective tissue. The fibrous structure, which consists of bundle of myocytes bound by collagen fibres, is modelled using a one-dimensional *Cosserat* continua. In the *Cosserat* continuum, every material point P is assigned a rotational field of displacements, enriching the continuum with

additional degrees of freedom. Additionally, a rotation tensor $\mathbf{R} \in SO(3)$, which is independent of the deformation gradient $\mathbf{F}$, is used to describe these degrees of freedom. In this way, two strain measures, a stretch-like strain tensor $\mathbf{U}$ and a change of curvature strain tensor $\mathbf{K}$, can be formulated as follows:

$$\mathbf{U} = \mathbf{R}^T\mathbf{F} \tag{3-1}$$

$$\mathbf{K} = -\frac{\mathbf{1}}{\mathbf{2}} \in : \left(\mathbf{R}^T\mathbf{F}_{,i}\right) \otimes \mathbf{V}_i \tag{3-2}$$

where the index $i = f, t, n$ and $\mathbf{V}_f, \mathbf{V}_t, \mathbf{V}_n$, illustrated in Figure 3-1, span an orthonormal basis describing fibre, sheet-tangent and sheet-normal directions, respectively.

A *Fung*-type orthotropic strain energy function $\psi(\mathbf{U}, \mathbf{K})$, which incorporates fibrous and complementary matrix components, is then defined as follows:

$$\psi(\mathbf{U}, \mathbf{K}) = \frac{1}{2} A \left(\mathrm{e}^{B[Q^{(s)}+Q^{(m)}]} - 1\right) + A_{comp}(J \ln(J) - J + 1) \tag{3-3}$$

where A, A_{comp} and B denote stress scaling coefficients; J is the Jacobian given by $J = \det(\mathbf{F})$, and the exponent Q is a function of the two strains weighted by material parameters assuming symmetry in the cross-fibre directions and defined by

$$Q^{(s)}\left(\mathbf{U}^{(s)}\right) = a_1 U_{ff}^2 + a_1\left(U_{tf}^2 + U_{nf}^2\right) + a_3 \frac{I_1}{A_f} K_{ff}^2 + a_4 \frac{I_2}{A_f}\left(K_{tf}^2 + K_{nf}^2\right) \tag{3-4}$$

$$Q^{(m)}\left(\mathbf{U}^{(m)}\right) = b_1(U_{tt}^2 + U_{nn}^2) + b_2\left(U_{ft}^2 + U_{fn}^2 + U_{nt}^2 + U_{tn}^2\right) \tag{3-5}$$

where $\mathbf{U}^{(m)} = \mathbf{U} \setminus \mathbf{U}^{(s)}$ is the part of $\mathbf{U}$ complementary to $\mathbf{U}^{(s)}$. Here $Q^{(s)}$ refers to strain energy contributions associated with the fibre bundle modelled by the *Cosserat* rod and $Q^{(m)}$ to those linked to the ECM. The material parameters a_i, referring to the tensile modulus, and b_i, to the shear modulus, govern the material anisotropy for the fibre and matrix, respectively.

In order to account for the transversely isotropic material behaviour, geometrical properties of the *Cosserat* rod were introduced. These properties are the circular cross-sectional area $A_f = \frac{\pi l^2}{4}$ and the second moments of areas linked to torsion and bending $I_1 = \frac{\pi l^4}{32}$ and $I_2 = \frac{\pi l^4}{64}$, respectively, which are functions of the characteristic length l. Furthermore, the cross-sectional area A_f of the fibre homogenises the strain energy representing the fibre continuum. From this perspective, the characteristic length is only

associated with the higher-order strain energy contributions in the change of curvature strain tensor **K**. Therefore, it controls the non-local influence towards a material point.

Finally, a corresponding variational principle was formulated as

$$\int_{\mathcal{B}} \{\boldsymbol{n} : \delta\mathbf{U} + \boldsymbol{m} : \delta\mathbf{K}\} dV - \mathcal{W}_{ext} = 0 \tag{3-6}$$

where $\boldsymbol{n} = \frac{\partial \psi}{\partial \mathbf{U}}$ is the force stress tensor, $\boldsymbol{m} = \frac{\partial \psi}{\partial \mathbf{K}}$ the couple stress tensor, and $\mathcal{W}_{ext}$ the external virtual work incorporating the heterogeneous response of all considered fibrous constituents.

3.4 Concluding remarks

This section summarised the constitutive model that is used within this study. The model is based on the *Cosserat* fibre continuum and was initially developed for cardiac tissues by Skatulla et al. (2014). Because cardiac and arterial tissues exhibit comparable mechanics, the model was found sufficiently adequate to reflect mechanical properties of arterial walls for a preliminary investigation. The defining feature of the model are characteristic scaling parameters which control the influence of higher-order strains arising from the relative motion of the micro-structural constituents.

However, it would be practically impossible to analytically analyse arterial walls using the presented constitutive model. Therefore, it is required that computational methods be employed for efficient and accurate analysis.

4. Computational analysis principles

4.1 Introduction

In Chapter 3, the *Cosserat* fibre continuum principles required in order to implement the constitutive model were briefly addressed. It was concluded that a computational analysis is required to apply the model to arterial walls. Thus, this section first provides a description of relevant considerations required when conducting computational analysis of arterial walls. Subsequently, the computational modelling techniques that are employed in this study are discussed, with methods of analysis being presented.

4.2 Nonlinear analysis

The type of analysis depends on the problem at hand. This study employs a nonlinear analysis because a finite strain and nonlinear material are used in the constitutive model.

4.3 Modelling method

Numerical modelling is a tool that is often used for engineering design and analysis (Rock et al., 2008). It solves physical problems making use of appropriate simplification of the reality. The simplification process requires that key variables be identified or introduced and relations between such variables be established. After the establishment of such variables and relations, it is common to construct a set of differential equations to be solved, thus allowing engineers to predict the outcomes of complex models and scenarios without conducting physical testing (Hopkins, 2014).

4.3.1 Finite Element Method

The increase in the complexity of structural designs caused by the continuous development of new structural materials has resulted in the need for careful and advanced analysis. Analytical techniques are still important today but numerical

methods have become an essential tool in the design process. The Finite Element Method (FEM) has been a fundamental procedure for the analysis of arterial walls. FEM is a technique applied to computational analysis in order to solve partial differential equations. An application of solving such equations is to predict the deformation and stress fields within solid bodies subjected to external forces such as concentrated and distributed loads. Moreover, FEM is the most widely used and appropriate method available to account for large changes in shape and non-linear material behaviour (Hopkins, 2014).

Three steps are usually used in FEM (Roylance, 2001): pre-processing, analysis and post-processing. During the pre-processing step, the creation of the material model takes place. The geometry of the model is discretised into so-called mesh elements with the assistance of various computer software programs. A finite element mesh is required in order to carry out a finite element analysis (Bower, 2009). With the finite element mesh, the geometry of the solid to be modelled can be specified and the displacement field within the solid can be described. Even with the use of meshfree methods described later in this section, a mesh is also required in order to discretise the geometry of the structure to be analysed. The mesh is created and defined by a set of nodes together with a set of finite elements, which as a whole represent the model to be analysed. In this regard, Bower (2009) describes a node as a discrete point within the solid body. The boundaries of elements within the body are represented by nodes. Moreover, this method applies the support and loading conditions to nodes. With the input geometry and boundary conditions, a dataset to be analysed is created.

The analysis of the model can be conducted following the pre-processing step. The dataset from the pre-processing step is used as input into the analysis. The input is then used to construct a set of linear or non-linear algebraic equations and solve them based on the fundamental equations of physics governing the problem (Hopkins, 2014). The general system of equations is given by:

$$\boldsymbol{K}\boldsymbol{u} = \overline{\boldsymbol{F}} \tag{4-1}$$

where the $\boldsymbol{K}$ is the stiffness matrix dependent on the type of problem to be analysed, $\boldsymbol{u}$ is the displacement matrix of nodes, and $\overline{\boldsymbol{F}}$ is the force matrix applied at nodes or upon elements bound by nodes in the case of line, traction, pressure and volume loads. Here,

it is possible to either solve for a matrix of unknown forces, or a matrix of unknown displacements (Roylance, 2001).

The post-processing step starts once the system of equations has been solved using numerical methods. Here the obtained results are interpreted. It is common that results are visualized using a post-processing software, which creates, for example, a coloured contour image of the initial or deformed body illustrating stress, strain, displacement, rotation and temperature (Roylance, 2001).

4.3.2 Element-Free Galerkin Method

The Element-Free Galerkin Method (EFGM) is a method used to solve equations. It solves set of differential equations by converting the governing set of equations to the weak form, known as the principle of virtual work, making use of moving least-squares interpolants (Belytschko et al., 1994).

EFGM was developed with the aim of reducing the computational time required for mesh generation. When utilising this method, the models to be analysed are free of any mesh, and only an array of nodes in the domain of consideration is required. Moreover, it presents the advantage that it does not seem to exhibit volumetric and shear locking (Belytschko et al., 1994). Thus EFGM is essential to this study in order to conduct analysis of three dimensional arterial walls, while avoiding volumetric and shear locking.

4.4 Implementation aspects

The implementation of the constitutive law was carried out by Dr Sebastian Skatulla, who is the supervisor of this study. The constitutive law was implemented within the SESKA framework. SESKA is a C++ code built upon by Dr Skatulla. The main software objective is to solve continuum mechanics problems utilising EFGM.

In this work, the analysis is carried out within SESKA. The geometry definition and 3D solution visualisation are handled using the pre- and post- processing commercial software package GiD. Most of the processes in SESKA are parallelised using a high

performance computer cluster (Hex cluster), in order solve large problem on high performance computers.

4.5 The variational formulation

This study EFGM is based on a variational formulation of the governing equations, also known as the principle of virtual work or the weak form (Sack, 2014). In continuum mechanics, the variational formulation states that the external potential $\mathcal{W}_{ext}$ is equal to the internal potential $\mathcal{W}_{int}$. The external potential refers to the work done by external forces acting on a non-linear boundary value problem in the domain $\mathcal{B}$. Thus the principle of virtual work is expressed as

$$\partial\psi = \mathcal{W}_{int} - \mathcal{W}_{ext} = 0 \tag{4-2}$$

where $\partial\psi$ is the variational formulation.

The internal potential is defined as

$$\psi_{(int)} = \int_{\mathcal{B}} \boldsymbol{S} : \delta\boldsymbol{E} dV = \int_{\mathcal{B}} \frac{1}{2}\boldsymbol{S} : \delta\boldsymbol{C} dV \tag{4-3}$$

where $\boldsymbol{S}$ denotes the second *Piola-Kirchhoff* stress tensor, $\boldsymbol{E}$ is the *Green strain* tensor, $\boldsymbol{C}$ is the right *Cauchy-Green* deformation tensor and the double dot operator $:$ denotes the scalar product of tensors.

$\boldsymbol{E}$ is defined as

$$\boldsymbol{E} = \frac{1}{2}(\boldsymbol{F}^T\boldsymbol{F} - 1) = \frac{1}{2}(\boldsymbol{C} - 1) \tag{4-4}$$

Thus the final variational formulation is defined as

$$\partial\psi = \int_{\mathcal{B}} \frac{1}{2}\boldsymbol{S} : \delta\boldsymbol{C} dV - \mathcal{W}_{ext} = 0 \tag{4-5}$$

4.6 Assembly of system of equations

The objective of assembling a system of equations is to obtain a discrete set of equations that can be solved for an unknown field, in particular displacement. Using Eq. (4-1), the following equation is obtained for linear problems

$$\boldsymbol{K}\,\Delta\boldsymbol{u} \;-\; [\boldsymbol{f}_{ext} - \boldsymbol{f}_{int}] = 0 \tag{4-6}$$

with $\boldsymbol{K}$ denoting the stiffness or tangent matrix, $\Delta\boldsymbol{u}$ the unknown displacement field increment, $\boldsymbol{f}_{ext}$ and $\boldsymbol{f}_{int}$ the external and internal loading and reaction vectors respectively.

Because this work deals with a nonlinear problem, an iterative procedure is required to solve for the unknown displacement field. In this regard, the Newton-Raphson method is utilised to find the unknown displacement field.

4.7 Concluding remarks

This chapter has dealt with the principles of computational analysis that are used in this study. Following this chapter, the attention is now paid to the computation of arterial walls using the computational software packages mentioned in this chapter: SESKA and GiD.

5. Numerical examples

5.1 Introduction

This chapter develops on problem definitions that are considered for the incorporation of circumferential residual stresses into the stress distribution of arterial walls under blood pressure. Therewith, a two-layer artery consisting of the media and adventitia is used. The intima is not considered as it has little influence on the mechanics of an artery, as reported in Section 2.3.1. Moreover, the influence of characteristic scaling parameters on the stress distribution is investigated through examples. Furthermore, this chapter provides the problem set-up and analysis of computational models, and presents corresponding results and discussions.

5.2 Problem definitions

Three problem definitions (Problem 1, 2 and 3) are developed for the incorporation of residual stresses in the circumferential stress distribution. They are derived from the opening angle method outlined in Section 2.5.2. In this method, an open artery is initially closed in order to obtain residual stresses acting on arterial walls in the load-free configuration. Thereafter, the stressed and load-free artery is put under blood pressure regime for the purpose of obtaining a circumferential stress distribution incorporating residual stresses.

However, this study only provides models of Problem 1 and Problem 3 for the purpose of investigation in the examples provided in Section 5.3. In this regard, Problem 2 is not modelled because of analysis limitations within SESKA, as later explained in Section 5.2.3.

5.2.1 Problem 1: Opened-up to closed configuration

This problem determines circumferential residual stresses that are acting within individual layers of the artery (media and adventitia). Herein the layers are modelled independently due to the fact that the size of the opening angle differs for individual arterial layers. With the aim to obtain residual stresses, the opened-up configuration of arterial layers are closed. These layers are closed by applying a displacement driven procedure over their cut surfaces. After closing the open arterial layers, the two closed configurations are regarded as residually stressed.

The geometrical data used for the size of opened-up arterial layers is obtained from Schröder and Hoegen (2015). It corresponds to an open sector of a circular cylindrical tube with opening angle α, wall thickness h, inner radius r_i and axial length L, as illustrated in Figure 5-1. Additionally, the angle β_f, which represents the angle between the two families of collagen fibres, is obtained from Holzapfel and Gasser (2007).

The material parameters of the two arterial layers are summarised in Table 5-1. They are of the *Fung*-type in accordance with the the constitutive model, but are not calibrated to experimental data. Furthermore, the values of parameters c_1 and c_4 are not provided in the table. This is because they represent the characteristic scaling parameters, of which the effect on the circumferential stress distribution is investigated in this study. Moreover, it is noteworthy that the relation between these parameters is $c_1 = 2c_4$, as reported in Section 3.3.1.

No loading condition is applied in this problem because the opened-up configuration of arterial layers is regarded as load-free and stress-free. On the other hand, geometrical *Dirichlet* boundary conditions are applied to the models. The application of these boundary conditions aims to obtain a displacement driven simulation closing the opened-up arterial layers and to ensure that the layers are sufficiently supported.

The assignment of *Dirichlet* boundary conditions over the open-up layers is shown in the problem setup-up depicted in Figure 5-1. These conditions are assigned over the two cut surfaces of each opened-up layer in order to close the artery in a rotational movement. This movement makes use of a rotation axis and rotation centre so that the two cut surfaces meet at half-distance when closing the layer. For both the media and adventitia, the rotation axis is the z-axis (0 0 1) and the rotation centre is the origin point (0.0 0.0 0.0). Additionally, a condition is assigned to the line across the middle of

the outer circumferential surface in order to provide the necessary support for analysis by ensuring that no displacement occurs in the z-direction along the line.

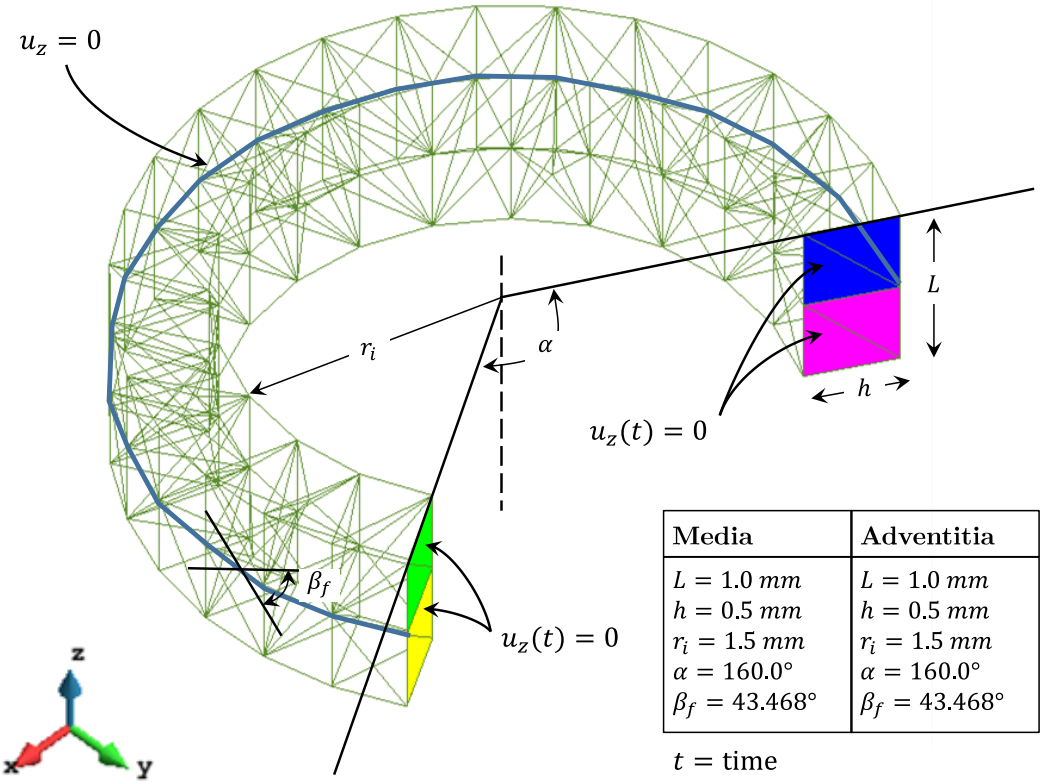

Figure 5-1: Problem set-up of the open configuration of arterial layers

Table 5-1: Non-calibrated material parameters for the media and adventitia

Layers	Bulk modulus/kPa	a_1/	a_2/	b_1/	b_2/	b_3/	b_4/	b_5/	b_6/	c_1/	c_4/
Media	$2.0e^1$	$3.0e^{-1}$	1.0	5.0	$1.0e^{-1}$	$1.0e^{-1}$	3.7	2.0	2.0	–	–
Adventitia	$2.0e^1$	$3.0e^{-1}$	1.0	5.5	$1.0e^{-1}$	$1.0e^{-1}$	3.7	2.0	2.0	–	–

The problem set-up is discretised for analysis, as illustrated in Figure 5-1. The discretisation results in 1250 mesh elements for the media and 1494 mesh elements for the adventitia, as detailed in Table 5-2.

Table 5-2: Mesh generated for Problem 1

Number of mesh elements		
Element type	**Media**	**Adventitia**
Linear	184	175
Triangular	410	429
Tetrahedral	456	656
Nodes	200	234

5.2.2 Problem 2: Closed configuration of the artery with residual stresses

This problem starts after the completion of the first problem. The latter only determines residual stresses acting within the two arterial layers, but ignores those acting at the interface surface between the layers. In this problem, residual stresses at the interface surface are determined, and the stress distribution incorporating residual stresses is obtained with the application of blood pressure.

Residual stresses at the interface surface are obtained by linking nodes of the media and adventitia at their interface surface. The linking of the two layers results in a closed artery, in which all the all the circumferential residual stresses are accounted for. Thereafter, a blood pressure of 13.33 kPa, which is assumed to be the mean arterial pressure, is applied over the inner surface of the closed artery in order to obtain the circumferential stress distribution. At the end of this problem, the circumferential stress distribution of at arterial walls incorporates circumferential residual stresses.

This problem is not modelled in the examples with this study because SESKA does not have the adequate implementation to simulate the linking process described above. However, the *Dirichlet* boundary and loading conditions that may be adequate for Problem 2 are outlined in Section 5.2.3.

5.2.3 Problem 3: Closed configuration of the artery without residual stresses

In this problem, the reference configuration is a load-free and stress-free two-layer artery, and only the blood pressure is applied to this configuration. This results in a circumferential stress distribution due to blood pressure, but ignoring the effect of residual stresses.

The problem model is a two-layer artery, which consists of the media and adventitia, and is assumed to be an ideal tube. The geometry of the model is obtained from Schröder and Hoegen (2015). It is defined by an inner radius $r_i = 1.0\,\text{mm}$, an outer radius $r_o = 2.0\,\text{mm}$ with both layers having a thickness of $h = 0.5\,\text{mm}$, and an axial length $L = 1.0\,\text{mm}$, as illustrated in Figure 5-2.

The artery is loaded by means of blood pressure of 13.33 kPa over the inner surface of the artery, as investigated by Holzapfel and Gasser (2006). The application of the loading is controlled by *Dirichlet* conditions such that the artery undergoes a user defined progressing displacement at the surface during each loading step. In this regard, a displacement increment is applied at each calculation step. However, the increment is only allowed to vary between 10^{-4} mm and 10^{-1} mm per calculation step, depending upon the number of iterations carried out before convergence of the global Newton-Raphson iteration of previous calculation steps.

The assignment of *Dirichlet* boundary conditions over the artery is shown in the problem setup-up depicted in Figure 5-2. These conditions are applied to the artery model with the aim of providing the necessary support, while ensuring that the model deforms symmetrically under loading conditions. Point displacement conditions are applied at three points located in the axial middle plane of the artery model, as illustrated in the problem-setup. They provide support to the model by ensuring that the expected displacements of the points occur during the deformation of the artery under blood pressure. In this regard, it is expected that the points move along the x-axis, but do not move in the y-axis and z-axis. Additionally, boundary conditions are applied to two lines in order to provide the necessary additional support required for the computational analysis of the model. The position of the two lines is shown in Figure 5-2. The line displacement boundary conditions ensure that the lines move in the x-axis direction, as expected, under the deformation caused by the blood pressure.

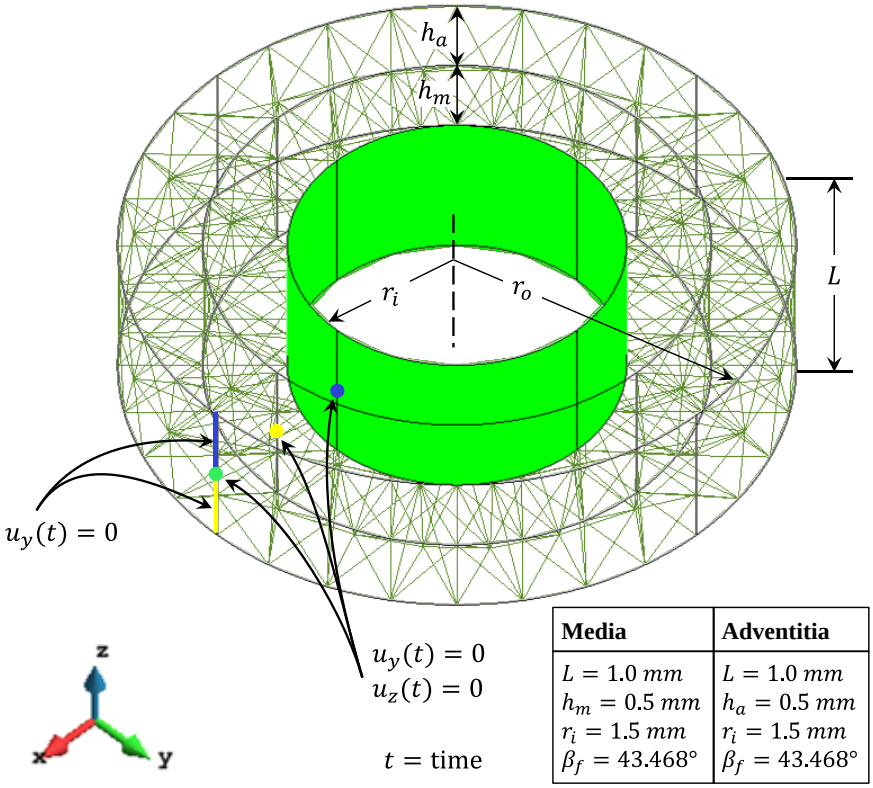

Media	Adventitia
$L = 1.0\ mm$	$L = 1.0\ mm$
$h_m = 0.5\ mm$	$h_a = 0.5\ mm$
$r_i = 1.5\ mm$	$r_i = 1.5\ mm$
$\beta_f = 43.468°$	$\beta_f = 43.468°$

Figure 5-2: Problem set-up of the stress-free closed configuration of the artery

Furthermore, this model is discretized into 4321 mesh elements, with the distribution of element types detailed in Table 5-3.

Table 5-3: Mesh generated for Problem 3

Number of mesh elements	
Element type	**artery**
Linear	294
Triangular	1127
Tetrahedral	2310
Nodes	590

5.3 Results

This section develops on examples which were used for investigation within this study, and the investigation results are also discussed. As mentioned above, the examples only cover Problem 1 and Problem 3. Additionally, the problem definitions were run with different characteristic scaling parameters c_1 and c_4, while keeping the parameters relation reported in Section 3.3.1. The following values of characteristic scaling parameters were used:

i) $c_1 = 1.0$ and $c_4 = 0.5$ (herein referred to as minimum parameter)

ii) $c_1 = 2.0$ and $c_4 = 1.0$ (herein referred to as middle parameter)

iii) $c_1 = 4.0$ and $c_4 = 2.0$ (herein referred to as maximum parameter)

The investigation was divided into two parts. The first part focused on investigating the proposed problem definitions for the incorporation of residual stresses. It provides contour plots and distribution graphs of the couple and force stresses using the middle-sized parameter. Here couple stress refers to circumferential stress and force stress to radial stress.

The second part puts the attention on the effect of characteristic scaling parameters on the arterial wall stress distributions. Here this effect was captured through graphs of the distribution of couple and force stresses over deformed arterial walls.

5.3.1 Characteristic scaling parameters: middle parameter

5.3.1.1 Results and discussions of Problem 1

Figure 5-3 and Figure 5-4 illustrate contour plots of the effective couple stress for the media and adventitia, respectively. They show that the media experiences the greatest tensile couple stress. Additionally the effective couple stress is tensile in both the media and adventitia.

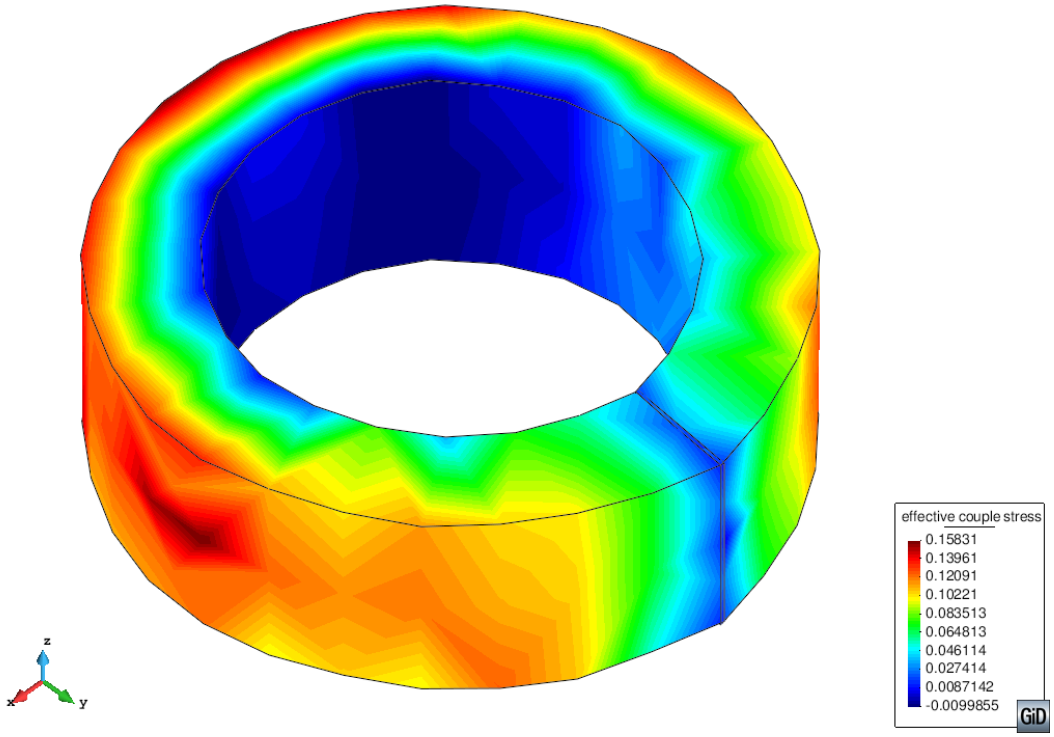

Figure 5-3: Effective **c**ouple stress contour plot of the closed media

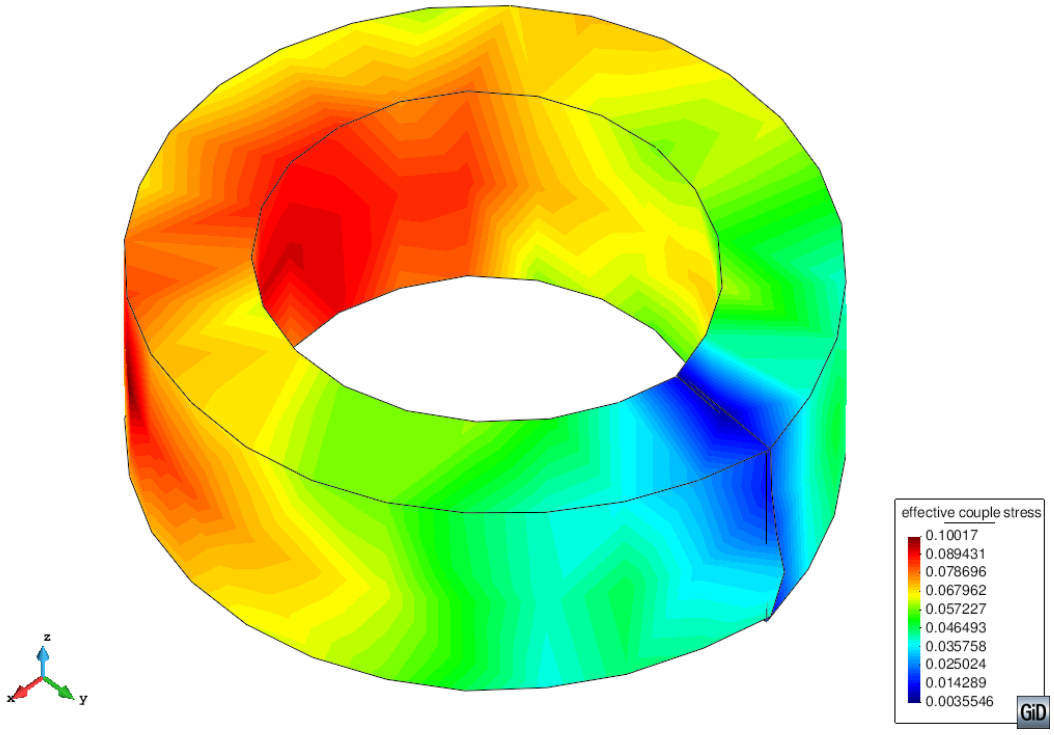

Figure 5-4: Effective **c**ouple stress contour plot of the closed adventitia

Contour plots of the effective force stress for the media and adventitia are illustrated in Figure 5-5 and Figure 5-6, respectively. They show that the adventitia experiences the greatest tensile effective force stress, while the media alone experiences compressive effective force stress.

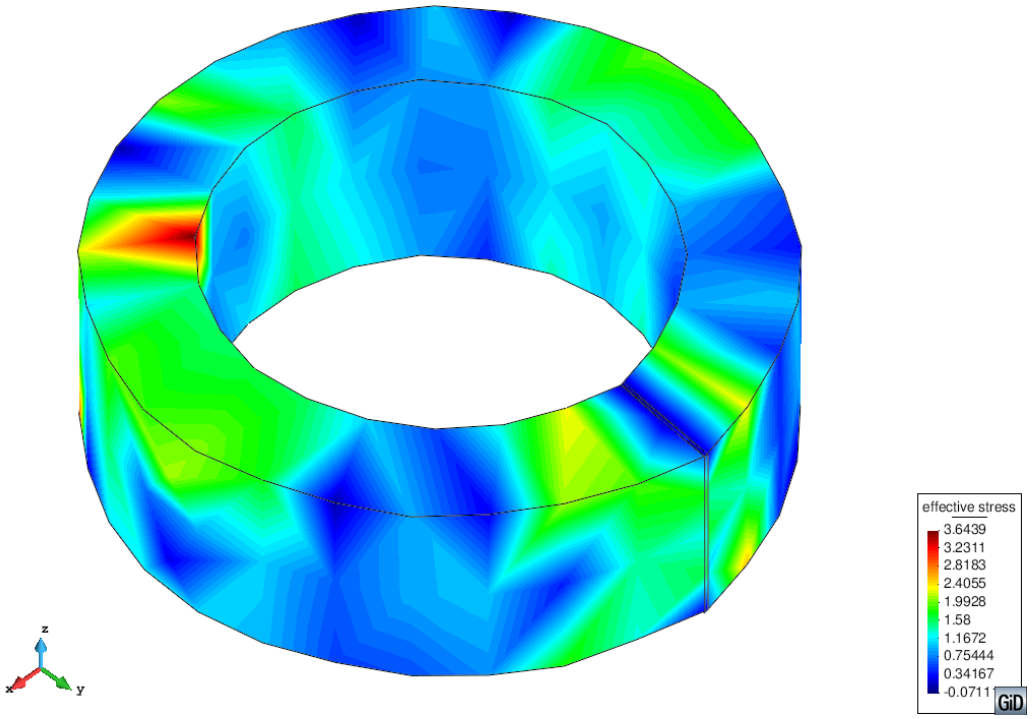

Figure 5-5: Effective force stress contour plot of the closed media

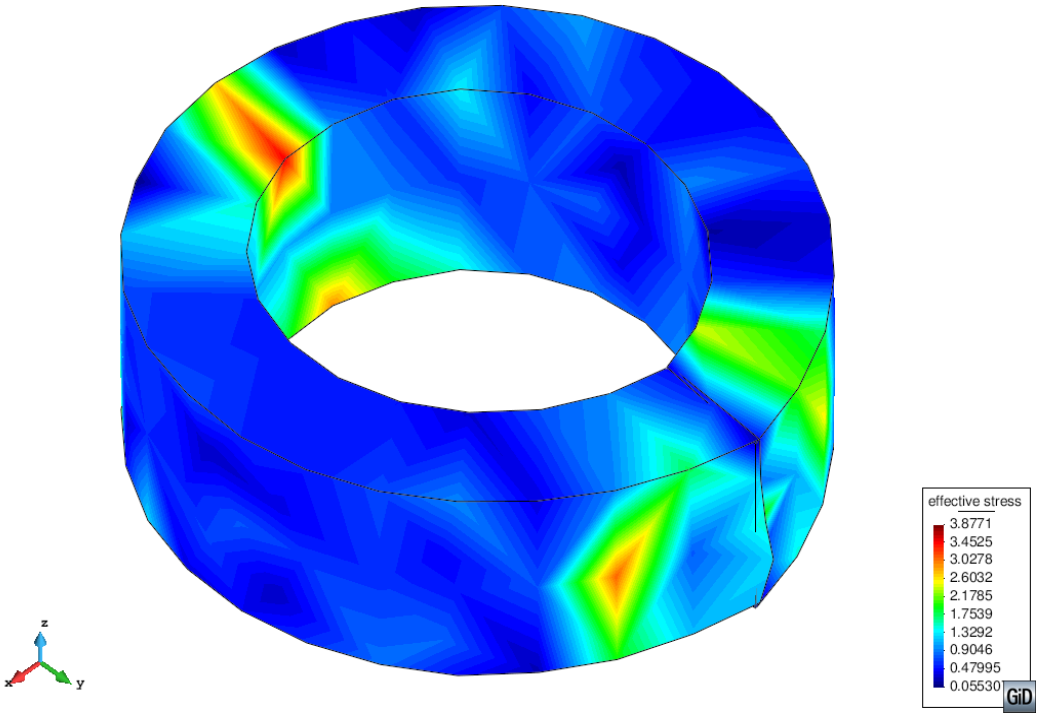

Figure 5-6: Effective force stress contour plot of the closed adventitia

For investigation, the stress distribution over the deformed wall is obtained at a vicinity that is equally influenced by the displacement of both cut surfaces. The position of this vicinity is illustrated in Figure 5-7.

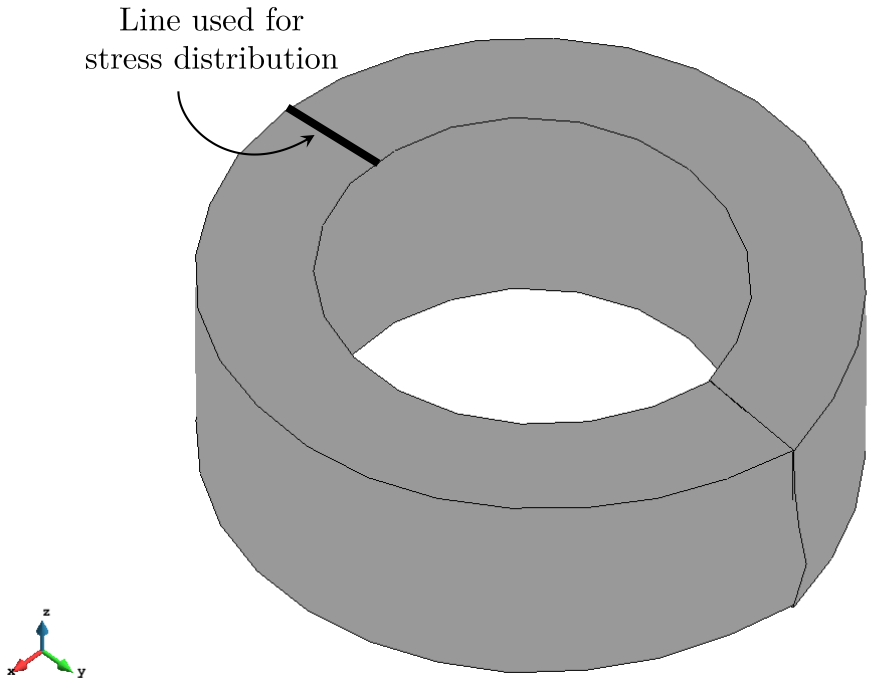

Figure 5-7: Radial line used for stress distribution over the deformed wall

Figure 5-8 and Figure 5-9 illustrate the effective couple stress distribution over the deformed wall of the media and adventitia, respectively. They show that effective couple stress increases from the inner to the outer surface of the media, while it decreases from the inner to the outer surface of the adventitia. Similarly to the observation on the contour plots in Figure 5-3 and Figure 5-4, the effective couple stress is tensile in both the media and adventitia.

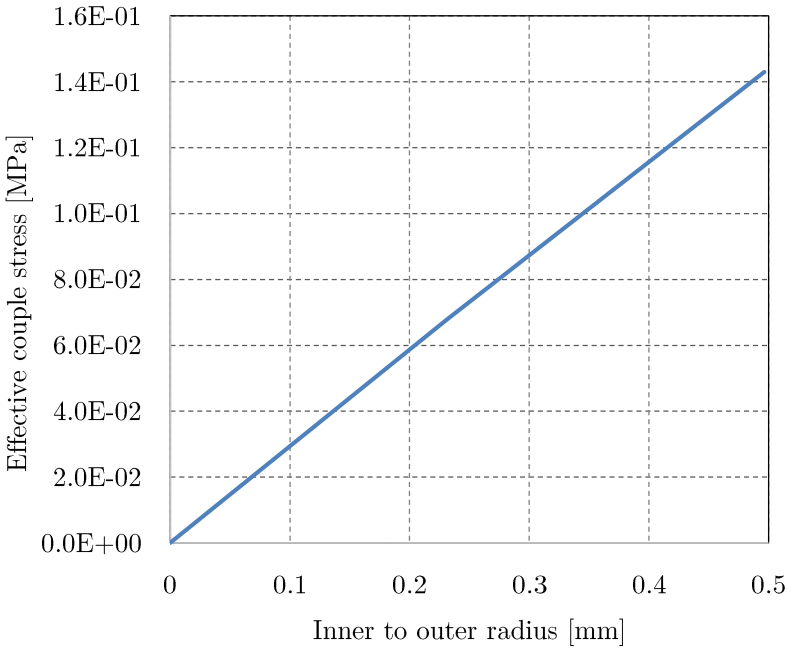

Figure 5-8: Effective couple stress distribution over the deformed wall of the media

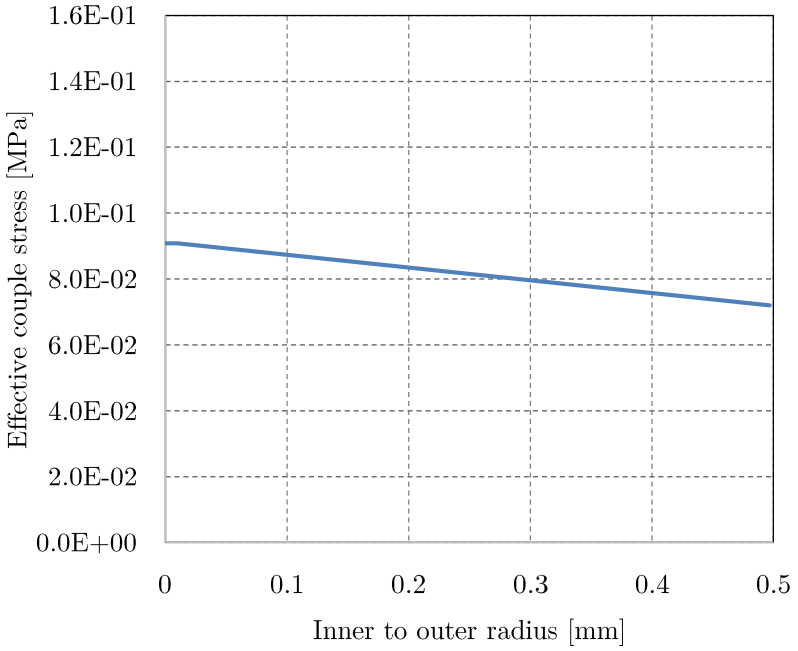

Figure 5-9: Effective couple stress distribution over the deformed wall of the adventitia

Figure 5-10 and Figure 5-11 depict the effective force stress distribution over the deformed wall of the media and adventitia, respectively. Figure 5-10 shows that the effective force stress gradient changes directions over the media. In this regard, the stress increases from the inner surface and then decrease towards the outer surface. However, the force stress at the outer surface is greater than at the inner surface. On the other hand, the effective force stress increases from the inner to the outer surface of the adventitia.

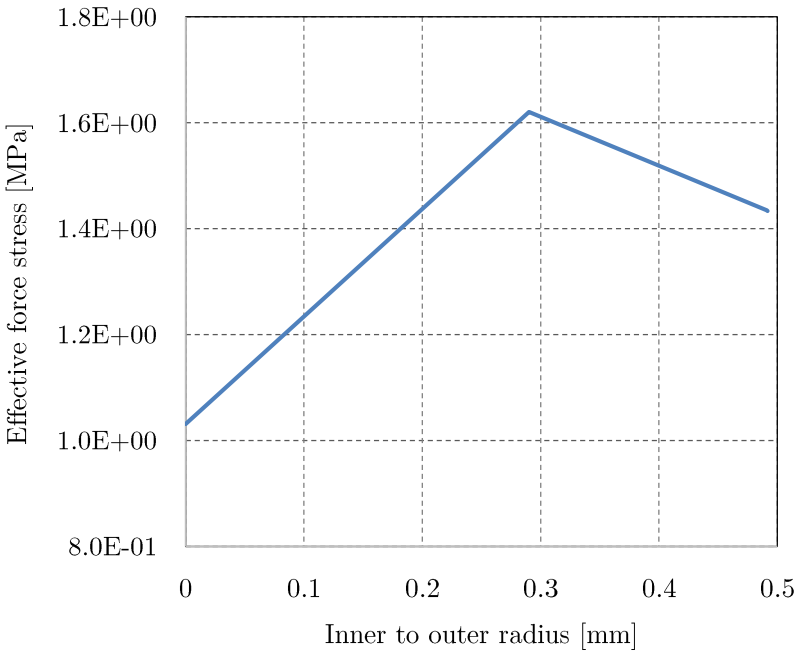

Figure 5-10: Effective force stress distribution over the deformed wall of the media

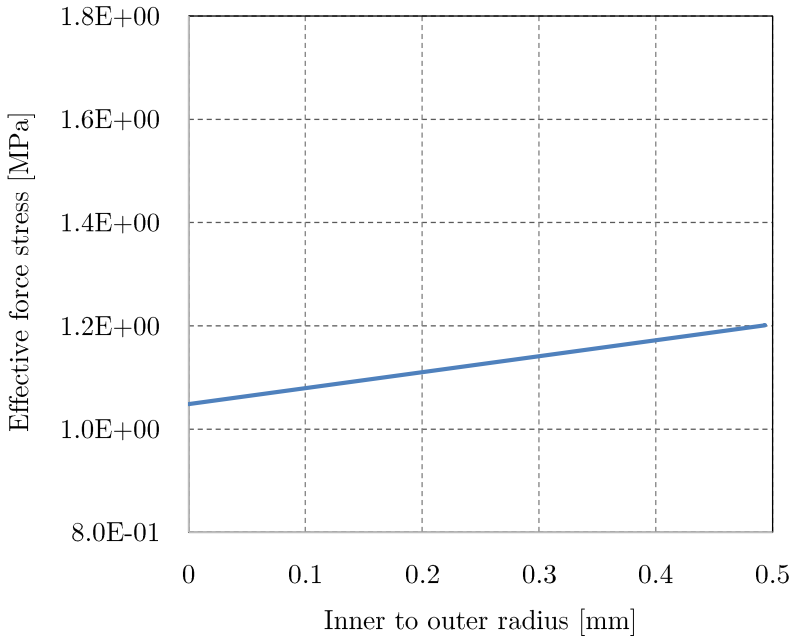

Figure 5-11: Effective force stress distribution over the deformed wall of the adventitia

5.3.1.2 Results and discussions of Problem 3

The contour plots, illustrated in Figure 5-12 and Figure 5-13, were obtained for the effective couple and force stresses of the stress-free artery under blood pressure. One can see that the effective couple stress tend to decrease from the inner surface to the outer surface of the artery. A similar trend can be observed on the effective force stress as it tends to decrease from the inner surface to the outer surface of the artery.

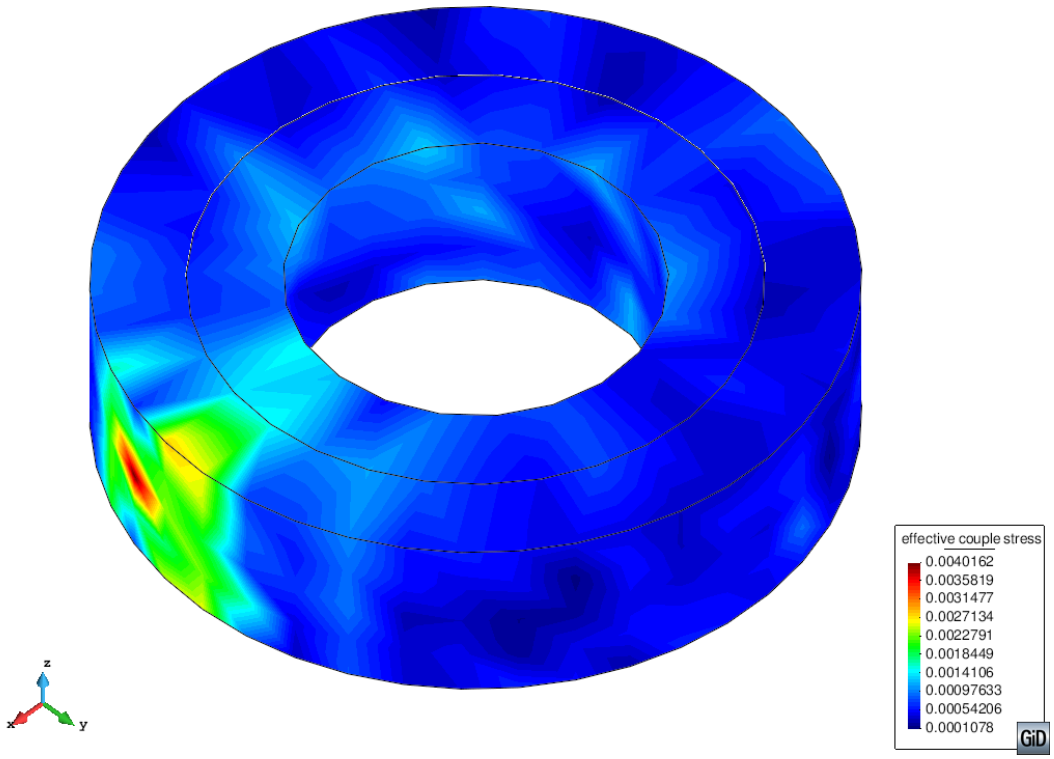

Figure 5-12: Effective couple stress contour plot of the artery

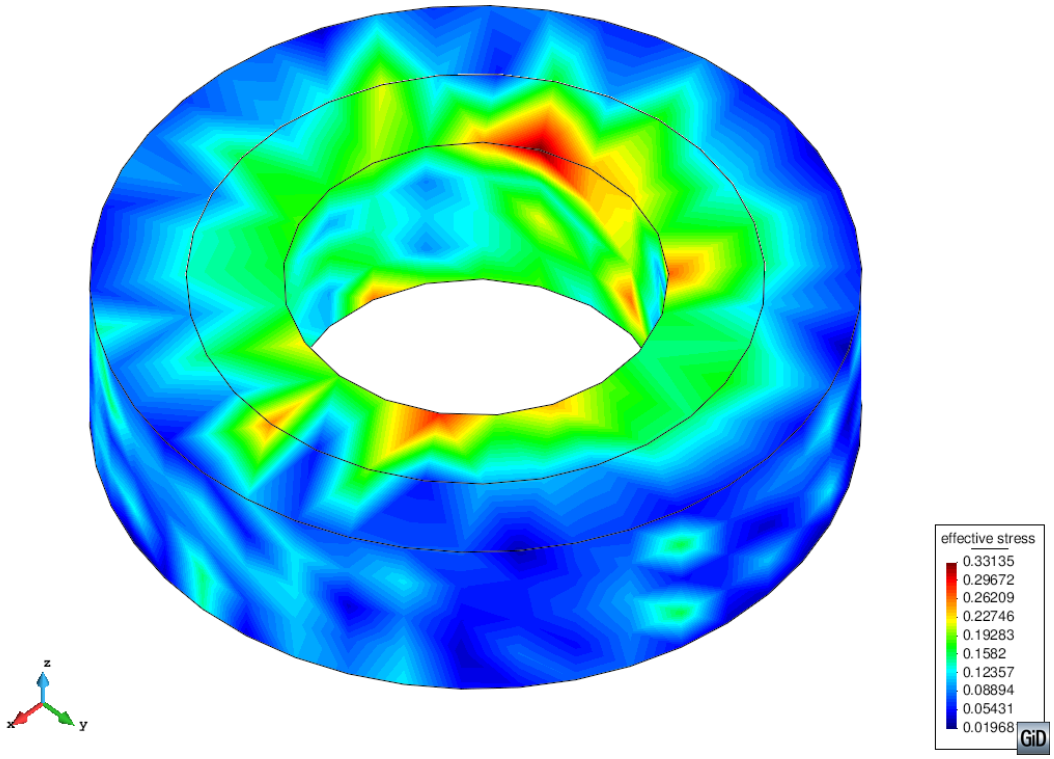

Figure 5-13: Effective force stress contour plot of the artery

Figure 5-14 shows the effective couple stress distribution over the deformed wall of the artery due to blood pressure. One can see that the effective couple stress is tensile through the artery. Moreover, it decreases from the inner to the outer surface of the media. On the other hand, it increases from the inner to the outer surface of the adventitia. Additionally, one can see that the stress is continuous at the interface between the media and adventitia.

However, the finding over the adventitia is in contradiction with the investigation of Holzapfel and Gasser (2006) which showed that the effective couple stress due to blood pressure is expected to decrease from the inner to the outer surface of the adventitia. Additionally, a discontinuity is expected between the interface between the media and adventitia.

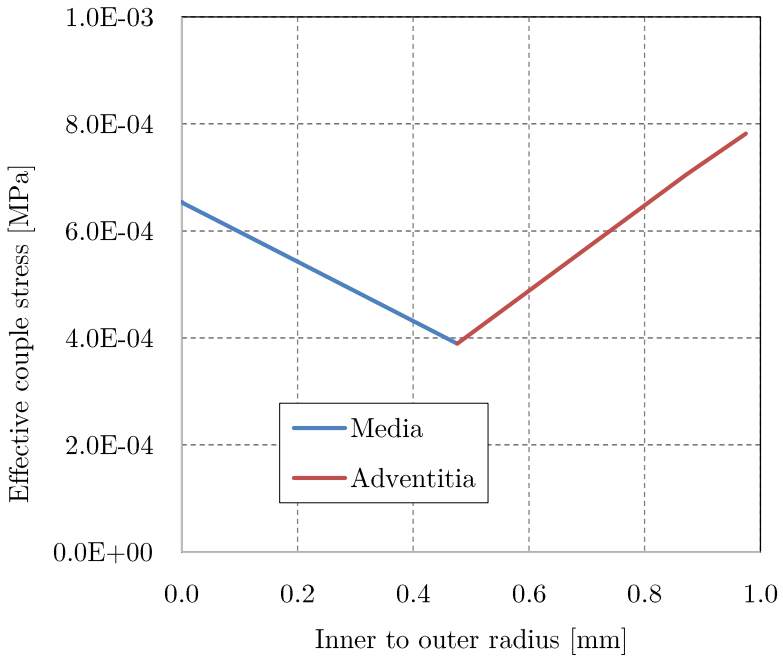

Figure 5-14: Effective couple stress distribution over the deformed wall of the artery

Figure 5-15 depicts the effective force stress distribution over the deformed wall of the artery. It can be seen that the effective force stress is decreasing from the inner to the outer surface of both the media and adventitia, with a greater reduction over the media. Additionally, one can see that effective force stress is tensile at the inner surface

and compressive at the outer surface of the media, while it is compressive over the adventitia.

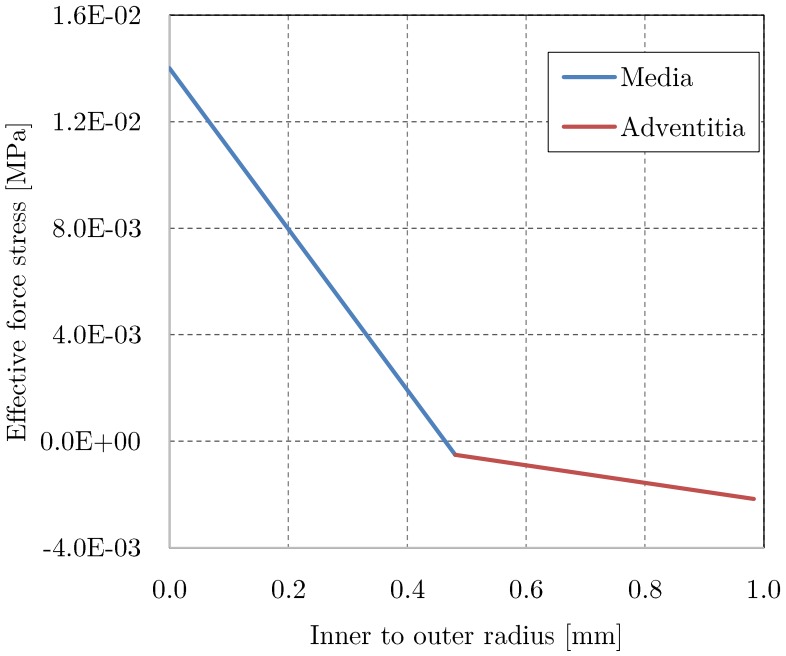

Figure 5-15: Effective force stress distribution over the deformed wall of the artery

5.3.2 Effect of characteristic scaling parameters c_1 and c_4

This section investigates the effect of the size of characteristic scaling parameters on the distribution of the couple and force stresses over deformed arterial walls. The results presented in this section are obtained from the simulations of Problems 1 and 3 with the three sizes of characteristic scaling parameters. as reported at the start of this chapter.

5.3.2.1 Results and discussions of Problem 1

The results of the effect of characteristic scaling parameters on the effective couple stress distribution over the media are shown in Figure 5-16. One does note that the minimum parameter has the highest stress at the inner surface, while the maximum parameter has the lowest stress at the inner surface of the media. Over this layer, the stress of the middle and maximum parameters increases, with the maximum parameter having a greater stress increase. However, the minimum parameter decreases instead over the media. This results in the effective couple stress of the minimum parameter being the

lowest at the outer surface, while the maximum parameter has the highest stress at the outer surface.

The results show that the size of the parameter influences the effective couple stress distribution over the media, but it is not possible to clearly define this influence. Moreover, it is possible that the result of the minimum parameter is an outlier as it does not follow the trend of the other two parameters.

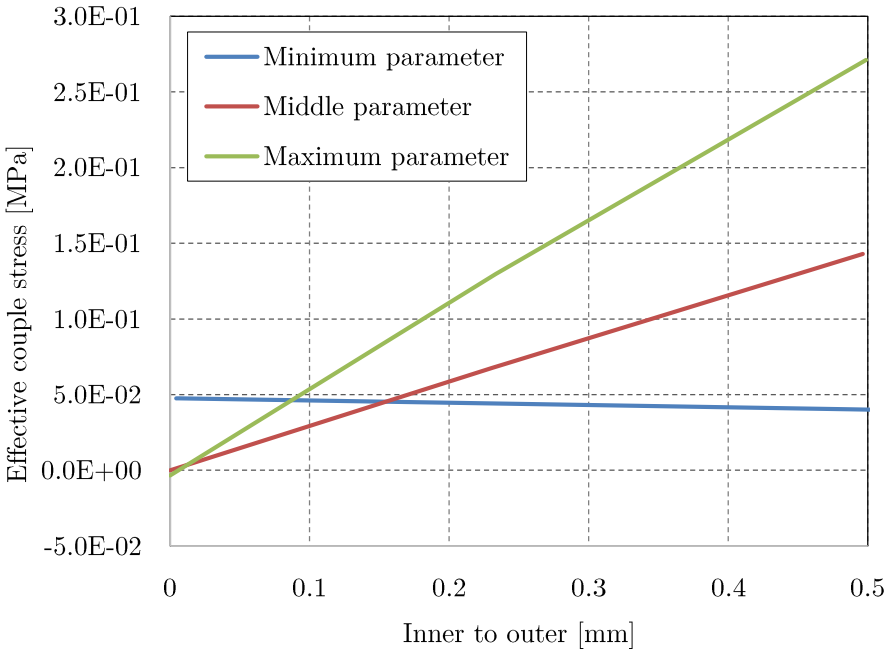

Figure 5-16: Effective couple stress distribution over the deformed wall of the media

Figure 5-17 illustrates the effective couple stress distribution over the adventitia. It shows that an increase in the size of parameters causes an increase of the effective couple stress over the adventitia. Moreover, the effective couple stress decreases from the inner to the outer surface of the adventitia for all parameters, but with different magnitudes. In this regard, the minimum parameter experiences the smallest stress decrease, followed by the middle parameter, and the maximum parameter which experiences the greatest stress decrease over the wall.

These results show that the increase in the size of parameters causes a decrease of the effective couple stress distribution in the adventitia. Additionally, the parameter size affects the stress decrease over the layer. In this regard, an increase in the size of parameters increases the stress decrease.

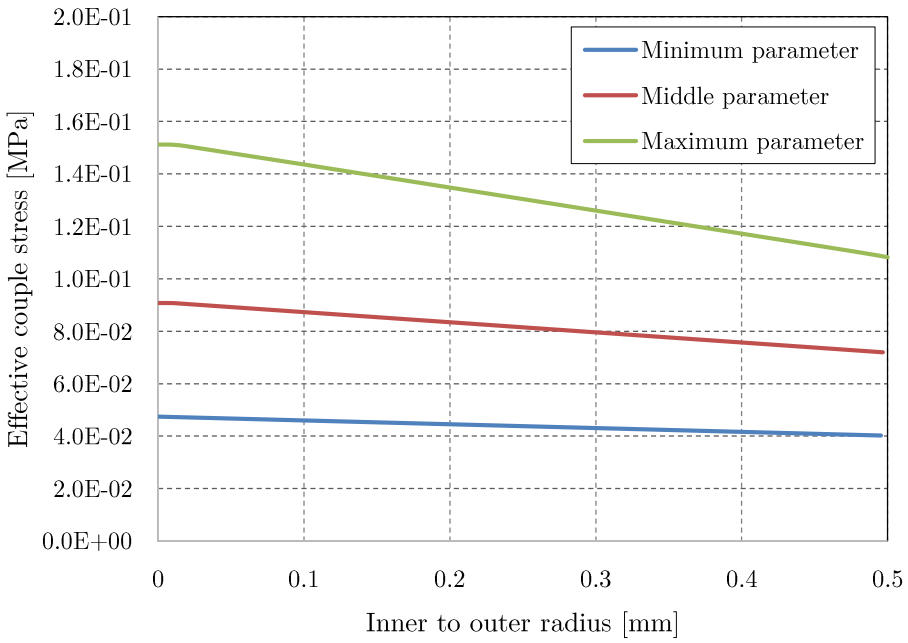

Figure 5-17: Effective couple stress distribution over the deformed wall of the adventitia

Figure 5-18 shows the effective force stress distribution over the media. It can be seen that the minimum parameter has the lowest stress at the inner surface, while the maximum parameter has the highest stress at the inner surface of the media. The stress of the minimum parameter increases from the inner to the outer surface in a straight line, whereas there is a change of gradient for the middle and maximum parameters. At the outer surface, the stress of the minimum parameter remains the lowest, while the stress of the middle parameter becomes the highest.

Similarly to the results of Figure 5-16, the size of the parameter is found to influence the effective force stress distribution over the media, but it is not possible to clearly define this influence.

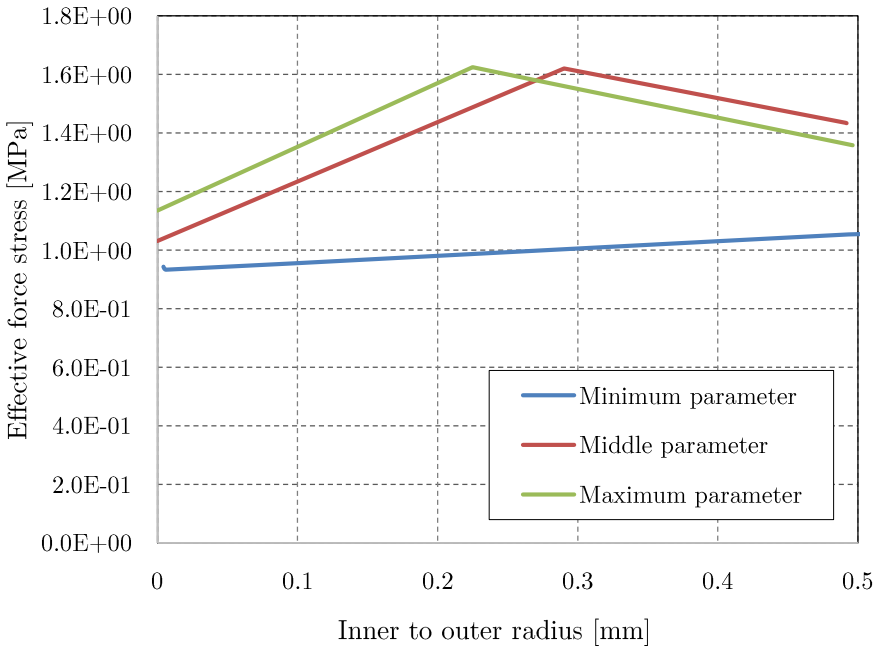

Figure 5-18: Effective force stress distribution over the deformed wall of the media

Figure 5-19 illustrates the effective force stress distribution over the adventitia. This illustration does not show a clear correlation between the size of parameters and effective force stress distribution. In this regard, one can see that the minimum parameter has the lowest force stress, while the middle parameter the highest. However, the stress gradient does not vary with parameter as it stays constant. Thus it is concluded that the size of parameter influence the effective force stress distribution, but that the influence is not clearly defined.

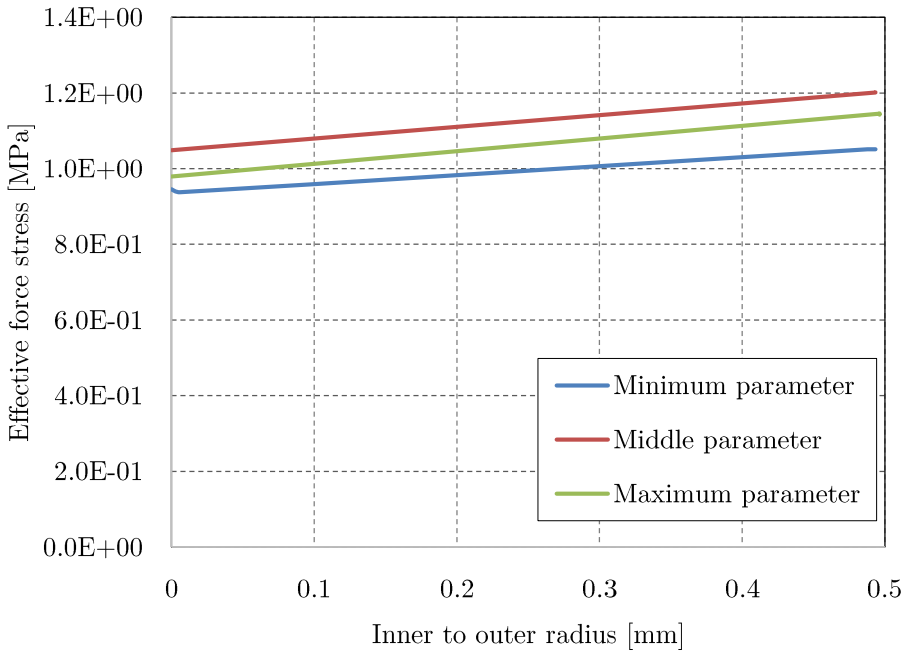

Figure 5-19: Effective force stress distribution over the deformed wall of the adventitia

5.3.2.2 Results and discussions of Problem 3

Figure 5-20 shows the effective couple stress distribution of the artery. Similarly to Figure 5-19, it does not provide a defined correlation between the size of parameters and effective couple stress distribution. In this regard, one can see that the stress of the middle parameter is the highest over the artery, while the maximum parameter stress is the lowest. Thus one can conclude that the parameter size influences the effective couple stress distribution with the available results, but this influence is not clearly defined.

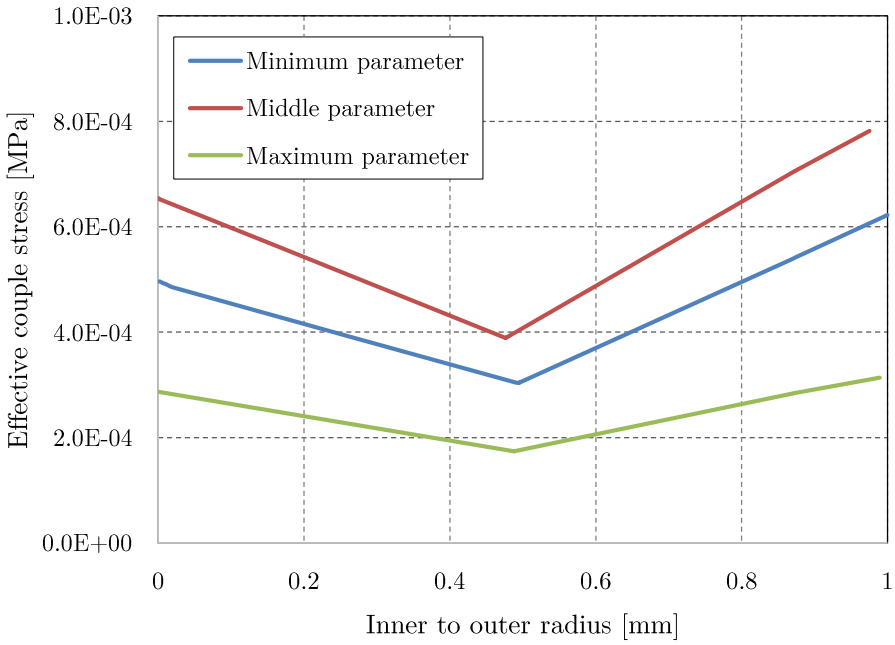

Figure 5-20: Effective couple stress distribution over the deformed wall of the artery

The effective force stress distribution over the artery is illustrated in Figure 5-21. Similarly to Figure 5-20, the illustration does not provide a defined correlation between the size of parameters and effective couple stress distribution. In this regard, one can see that the stress of the middle parameter is the lowest, while the minimum parameter stress is the highest. Thus it is also concluded that that the size of parameters influence the effective force stress distribution, but that the influence is not clearly defined.

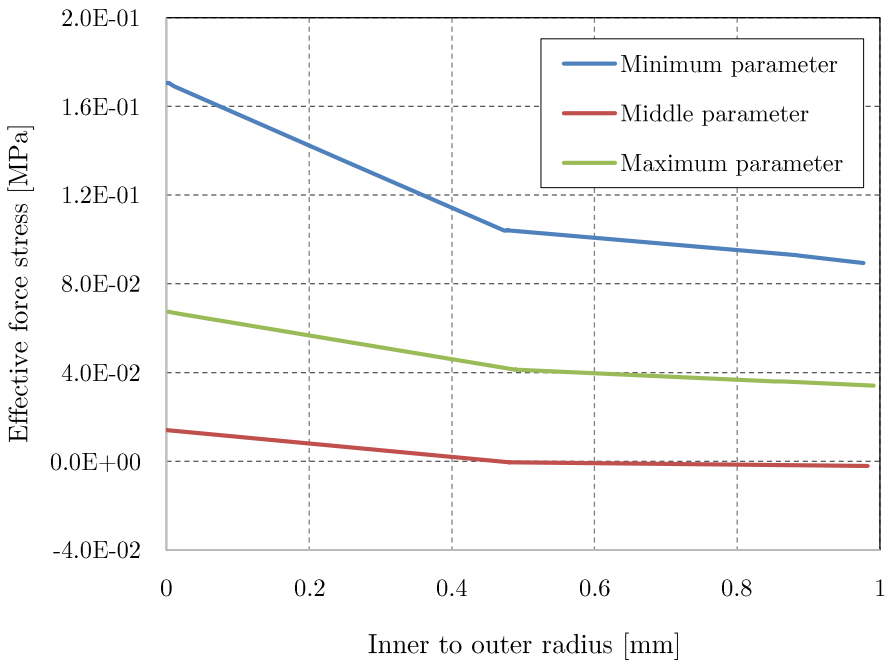

Figure 5-21: Effective force stress distribution over the deformed wall of the artery

5.4 Concluding remarks

This section presented the problem definitions that are proposed for the incorporation of residual stresses and investigation of effect of characteristic scaling parameters over the distribution of effective couple and force stresses. In this regard, it was reported that the investigation results are qualitative as model parameters are not calibrated to experimental data, and that analysis implementations could not be achieved for all problem definitions within this study timeline.

With regard to the incorporation of circumferential residual stresses, it was found that these stresses increase from the inner to the outer surface of the media, but decrease from the inner to the outer surface of the adventitia. Moreover, they were found to be tensile over both arterial layers. On the other hand, circumferential stresses due to blood pressure were found to decrease from the inner to the outer surface of the media, while they increase from the inner to the outer surface of the adventitia. Additionally, they were also found to be tensile over the artery. The results also showed that there is no stress discontinuity at the interface surface between the media and adventitia. Furthermore, it can be qualitatively concluded that circumferential residual stresses tend to

decrease the stress gradient over the media, while they tend to increase it over the adventitia, with respect to stress gradient directions in individual arterial layers and artery.

However, some of the results were found to be in contradiction with findings in the literature review. In this regard, circumferential residual stresses were expected to be compressive on the inner surface and tensile on the outer surface of both the media and adventitia. Moreover, circumferential stresses due to blood pressure were expected to decrease from the inner to the outer surface of the adventita, as illustrated in Figure 2-4. Furthermore, a stress discontinuity was expected at the surface interface between the media and adventita. Additionaaly, it was expected that circumferential residual stresses tend to reduce the stress gradient over the adventitia

With regard to the effect of characteristic scaling parameters, it was concluded that these parameters influence the magnitude and gradient of the distribution of couple and force stresses. However, the results were found to be inconclusive in order to clearly define this influence.

6. Conclusions and recommendations

The focus of this study was to develop a model incorporating circumferential residual stresses in arterial walls and to investigate the effect of characteristic scaling parameters of the *Cosserat* fibre continuum model on the stress distribution. This chapter summarises the major findings, acknowledge the study shortcomings and outline future studies for research.

6.1 Summary and general concluding remarks

This document began with an introduction into the study by providing the reader with background information on the topic. Subsequently, the research motivation and importance were presented. Thereafter, the aims and objectives of the study were provided, together with the scope and limitation. This was followed by a literature review which expanded on properties of residual stresses, mechanics of arterial walls, the procedure for parameter identification, and the method of incorporation of circumferential residual stresses in arterial walls.

The material of arterial walls was modelled using the *Cosserat* fibre continuum. This constitutive model was initially developed for cardiac tissues, nonetheless it can also be used for a preliminary investigation on arterial tissues as these two types of tissue exhibit comparable mechanics. Moreover, the model is defined by characteristic scaling parameters, of which the influence on the wall stress distribution is investigated in this study.

The opening-angle method was employed for the incorporation of circumferential residual stresses. This method requires the consideration of an open artery, which is assumed to be stress-free. Here the medial and adventitial layers are considered independently because they have different opening angles. The open arterial layers are initially closed in order to obtain circumferential residual stresses acting within individual arterial layers in the load-free configuration. The stressed and load-free layers are then linked in order to form a closed artery and account for circumferential residual stresses acting at the interface surface between layers. Thereafter, the blood pressure is applied

in order to obtain a wall stress distribution incorporating circumferential residual stresses.

For the computational simulation of arterial walls, two computational software packages were used: SESKA and GiD. SESKA was used for the computational analysis of models, while GiD was used for the pre- and post- processing of models. However, SESKA presented some limitations as it could not implement the linking procedure of individually stressed arterial layers, which is required to account for residual stresses at the interface surface. As a consequence, this procedure was not carried out in this study. Hence simulations results only determine circumferential residual stresses acting within arterial layers and circumferential stresses due to blood pressure in a stress-free artery. Moreover, model parameters of arterial layers were not calibrated to the available experimental data because the calibration could not be achieved within this study timeline. Therefore, only qualitative results were obtained in this investigation.

The investigation on the incorporation of circumferential residual stresses showed both satisfactory and contradictory results. On the satisfactory results, residual stresses were found to reduce the stress gradient over the media. Furthermore, circumferential stresses due to blood pressure were found to decrease from the inner to the outer surface of the media. Additionally, these stresses were found to be tensile over the artery.

In contrast to the literature review, circumferential residual stresses were found to increase the stress gradient over the adventitia instead of reducing it. Moreover, they were expected to be compressive on the inner surface and tensile on the outer surface of both the media and adventitia, but were found to be tensile over both layers. Furthermore, circumferential stresses due to blood pressure were expected to decrease from the inner to the outer surface of the adventita, bu they were to be increasing in that direction. Furthermore, a stress discontinuity was expected at the surface interface between the media and adventita, but the stress was found to be continuous in the investigation.

The investigation into the effect of characteristic scaling parameters found that these parameters do influence the magnitude and gradient of the distribution of effective couple and force stresses. However, the results were found to be inconclusive for a clear definition of this influence.

In conclusion, this study can be used as a preliminary investigation as some results were found satisfactory. Additionally, the investigation method has been widely used with satisfactory results in past studies. However, further investigation is required in order to obtain the results that are satisfactory and conclusive. In this regard, the next section provides the areas that should be improved in future studies.

6.2 Further studies

Incorporation of circumferential residual stresses

Further investigation is recommended in order to incorporate circumferential residual stresses with the aim of obtaining satisfactory results. This investigation should include the linking procedure so that circumferential residual stresses are accounted for at the interface surface between arterial layers. Moreover, the constitutive model needs to be adapted to arterial tissues in order to better capture their mechanical behaviour. Additionally, the calibration of model parameters to experimental data is required in order to obtain a quantitative and quantitative results.

Effect of characteristic scaling parameters

The investigation within this study on the effect of characteristic scaling parameters over the wall stress distribution confirmed that these parameters influence the stress distribution. However, this influence could not be successfully defined due to the limited investigation data. Thus it is recommended that more sizes of parameters be used in future studies in order to clearly define the influence of parameters on the stress distribution.

7. List of references

Abè, H., Hayashi, K. & Sato, M., 1996. *Data book on mechanical properties of living cells, tissues, and organs.* New York: Springer.

Alaslrué, V. et al., 2007. Assessing the use of the ''opening angle method" to enforce residual stresses in patient-specific arteries. *Ann. Biomed. Eng.,* pp. 1821-1837.

Alastrué, V., Martinez, M. A. & Doblaré, M., 2008. Modelling adaplive volumetric finite growth in patient-specilic residually stresses arteries. *J. Biomech.,* Volume 41, pp. 1773-1781.

Alastrué, V., Martinez, M. A., Doblaré, M. & Menzel, A., 2009. Anisotropic micro-sphere-based finite elasticily applied to blood vessel modelling. *J. Mech. Phys. Solids,* Volume 57, pp. 178-203.

Alford, P. W., Humphrey, J. D. & Taber, L. A., 2008. Growth and remodeling in a thick-walled artery model: effects or spatial variations in wall constituents. *Biomech. Model. Mechanobiol,* 7(4), pp. 245-262.

Azeloglu, E. U. et al., 2008. Heterogeneous transmural proteoglycan distribution provides a mechanism for regulating residual stresses in the aorta. *American Journal of Physiology – Heart and Circulatory Physiology,* Volume 294, pp. Hl197-H1205.

Balzani, D., Brinkhues, S. & Holzapfel, G. A., 2012. Constitutive framework for the modeling of damage in soft biological tissues. *Comput. Methods Appl. Mech. Eng.,* Volume 213-216, pp. 139-151.

Balzani, D., Schröder, J. & Grossa, D., 2005. Numerical simulation of residual stresses in arterial walls. *Computational Materials Science,* 39(1), pp. 117-123.

Balzani, D., Schroder, J. & Gross, D., 2006. Simulation of discontinuous damage incorporating residual stresses in circumferentially overstretched atherosclerotic arteries. *Acta Biomater,* Volume 2, pp. 609-618.

Belytschko, T., Lu, Y. Y. & Gu, L., 1994. Element-Free Galerkin Methods. *International Journal for Numerical Methods in Engineering,* p. 37229.

Bergel, D. H., 1960. *The visco-clastic properties of the arterial wall. PhD thesis.* London: University of London.

Block, P. C., 1984. Mechanism of transluminal angioplasty. *Am. J. Cardiol,* Volume 53, pp. 69C-71C.

Bower, A., 2009. *Applied mechanics of solids.* United States of America: CRC Press.

Brinkhues, S., 2012. *Modeling and simulation of arterial walls with focus on damage and residual stresses,* Essen: Universit¨at Duisburg-Essen.

Bustamante, C. & Holzapfel, G. A., 2010. Methods to compute 3D residual stress distributions in hyperelastic tubes with application to arterial walls. *lnt. J. Eng. Sci.,* 48(11), pp. 1066-1082.

Canfield, T. R. & Dobrin, P. B., 2007. *Mechanics of Blood Vessels,* Illinois: Argonne National Laboratory.

Cardamone, L., Valentin, A., Eberth, J. F. & Humphrey, J. D., 2009. Origin of axial prestretch. *Biornechanics and Modeling in Mechanobiology,* Volume 8, pp. 431-446.

Cardamone, L., Valentin, A., Eberth, J. F. & Humphrey, J. D., 2009. Origin of axial prestretch and residual stress in arteries. *Biomech. Model. Mechanobiol.,* Volume 8, pp. 431-446.

Carew, T. E., Vaishnav, R. N. & Patel, D. J., 1968. Compressibility of the arterial wall. *Circ. Res.,* Volume 23, pp. 61-68.

Chaudhry, H. R. et al., 1997. Residual stresses in oscillating thoracic arteries reduce circumferential stresses and stress gradients. *J. Biomech,* Volume 30(1), pp. 57-62.

Cheng, G. C. et al., 1993. Distribution of circumferential stress in ruptured and stable atherosclerotic lesions. A structural analysis with histopathological correlation. *Circulation,* Volume 87, pp. 1179-1187.

Cheng, W. & Finnie, I., 2007. *Residual Stress Measurement and the Slitting Method.* s.l.:Springer US.

Chen, Y. C. & Eberth, J. F., 2012. Constitutive function. residual stress, and state of uniform stress in arteries. *J. Mech. Phys.,* 60(6), pp. 1145-1157.

Chuong, C. J. & Fung, Y. C., 1983. Three-dimensional stress distribution in arteries. *J. Biomech. Eng.,* Volume 105, pp. 268-274.

Chuong, C. J. & Fung, Y. C., 1984. Compressibility and constitutive equation of arterial wall in radial compression experiments. *J. Biomech.,* Volume 17, pp. 35-40.

Chuong, C. J. & Fung, Y. C., 1986. On residual stress in arteries. *J. Biomech. Eng,* Volume 108, pp. 189-191.

Dobrin, P. B. & Canfield, T. R., 1984. Elastase, collagenase, and the bi-axial elastic properties of dog carotid artery. *Am. J. Physiol.,* Volume 2547, pp. H124-H131.

Dobrin, P. B., Mrkvicka, R. & Schwarcz, T. H., 1990. Longitudinal rctractive force in pressurized dog and human arteries. *J. Surg. Res.,* Volume 48, pp. 116-120.

Dobrin, P. B. & Rovick, A. A., 1969. Influence of vascular smooth muscle on contractile mechanics and elasticity of arteries. *Am. J. Physiol.,* Volume 217, pp. 1644-1651.

Famaey, N., Vander Sloten, J. & Kuhl, E., 2013. A three-constituent damage model for mterial clamping in computer-assisted surgery. *Biomech. Model. Mechanobiol.,* 12(1), pp. 123-136.

Fatemi, J., Van Keulen, F. & Onck, P., 2002. Generalized continuum theories: Application to stress analysis in bone. *Meccanica,* 37(4-5), p. 385–396.

Fomovsky, G. M., Thomopoulos, S. & Holmes, J. W., 2010. Contribution of extracellular matrix to the mechanical properties of the heart. *J Mol Cell Cardiol,* 48(3), pp. 490-496.

Fuchs, R. F., 1900. Zur Physiologie und Wachstumsmechanik des Blutgefaßsystems. *Arch. Ges. Physiol,* Volume 28.

Fung, Y. C., 1991. Whal are the residual stresses doing in our blood vessels?. *Ann. Bio med. Eng.,* Volume 19(3), pp. 237-249.

Fung, Y. C., 1993. *In Biomechanics: mechanical properties of living tissue.* 2nd ed. New York: Springer.

Fung, Y. C. & Liu, S. Q., 1989. Change of residual strains in arteries due to hypertrophy caused by aortic constriction. *Circ. Res.,* Volume 65, pp. 1340-1349.

Gasser, C. T., Ogden, R. W. & Holzapfel, G. A., 2006. Hyperelastic modelling of arterial layers with distributed collagen fibre orientations. *J. R. Soc. Interface,* Volume 3, pp. 15-35.

Gasser, T. C. & Holzapfel, G. A., 2002. A rate-independent elastoplastic constitutive model for (biological) fiber reinforced composites at finite strains: continuum basis algorithmic formulation and finite element implementation. *Comput. Mech.,* Volume 29, pp. 340-360.

Greenwald, S. E. et al., 1997. Experimental investigation of the distribution of residual strains in the artey wall. *J. Biomech. Eng,* Volume 119, pp. 438-444.

Holzapfel, G. A., 2001. Biomechanics of soft tissue. *The handbook of materials behavior models,* Volume 3, pp. 1049-1063.

Holzapfel, G. A. & Gasser, T. C., 2006. Computational stress-deformation analysis of arterial walls including high-pressure response. *Int. J. Cardiol,* Volume 116, pp. 78-85.

Holzapfel, G. A. & Gasser, T. C., 2006. Computational stress-deformation analysis of arterial walls including high-pressure response. *Int. J. Cardiol,* Volume 116, pp. 78-85.

Holzapfel, G. A., Gasser, T. C. & Ogden, R. W., 2000. A new constitutive framework for arterial wall mechanics and a comparative study of material model. *J. Elast.* , Volume 61, pp. 1-48.

Holzapfel, G. A., Gasser, T. C. & Stadler, M., 2002a. A structural model for the viscoelastic behavior of arterial walls: continuum formulation and finite element analysis. *Eur. J. Mech. A/Solids,* Volume 21, pp. 441-463.

Holzapfel, G. A. & Ogden, R. W., 2010. Modelling the layer-specific 3d residual stresses in arteries, with an application to the human aorta. *J. R. Soc. llllerrace,* Volume 7, pp. 787-799.

Holzapfel, G. A. et al., 2007. Layer-specific 3d residual deformations of human aortas with non-athc rosclerotic intimal thicke ning. *Ann. Biomed. Eng.,* 35(4), pp. 530-545.

Holzapfel, G. A., Sommer, G. & Regitnig, P., 2004. Anisotropic mechanical properties of tissue components in human atherosclerotic plaques. *J. Biomech. Eng.,* Volume 126, pp. 657-665.

Hopkins, G., 2014. *Highly Non-linear Post-buckling Analysis of Shell Structures,* Cape Town: University of Cape Town.

Humphrey, J. D., 2002. *In Cardiovascular solid mechanics Cells, tissues, and organs.* New York: Springer.

Huyghe, J. M., Arts, T., van Kampen, D. H. & Reneman, R. S., 1992. Porous medium finite element model or the beating left ventricle. *Am. J. Phys.,* Volume 262,, pp. Hl 256- H1 267.

Huyghe, J. M., van Kampen, D. H., Arts, T. & Hcethaar, R. M., 1991. The constitutive behaviour of passive heart muscle tissuE: a quasi-linear viscoelastic formulation. *J. Biomech,* Volume 24, pp. 841-849.

Klarbring, A., Olsson, T. & Stahlhand, J., 2007. Theory of residual stresses with application to an arterial geometry. *Arch. Mech.,* 59(4-5), pp. 341-364.

Lanir, Y., 2009. Mechanisms of residual stress in soft tissues. *J. Biomech. Eng.,* 31(044506), pp. 1-5.

Lanir, Y., 2012. Osmotic swelling and residual stress in cardiovascular tissues. *J. Biomech,* Volume 45, pp. 780-789.

Liu, S. Q. & Fung, Y. C., 1988. Zero-stress states of arteries. *J. Biomech. Eng.,* Volume 110, pp. 82-84.

Liu, S. Q. & Fung, Y. C., 1989. Relationship between hypertension, hypertrophy, and opening angle of zero-stress state or arteries following aortic constriction. *J. Biomech. Eng.,* Volume 111, pp. 325-335.

Li, Z. Y. et al., 2006. Stress analysis of carotid plaque rupture based on in vivo high resolution lVIRI. *Journal of Biomechanics,* Volume 39, pp. 2611-2622.

Mase, G. E., 1999. *Continnum mechanics for engineers.* New York: CRC Press.

Mase, T. G. & Mase., G. E., 2010. *Continuum mechanics for engineers.* s.l.:Crc Press.

Matsumoto, T., Goto, T., Furukawa, T. & Sato, M., 2004. Residual stress and strain in the lamell arunit of the porcine aorta: experiment and analysis. *J. Biomech.,* 37(6), pp. 807-815.

Menzel, A., 2007. A fibre reorientation model for orthotropic multiplicative growth. *Biomech. Model. Mcchanobiol.,* Volume 6, pp. 303-320.

Munch, I., Neff, P. & Wagner, W., 2011. Transversely isotropic material: nonlinear cosserat versus classical approach. *Continuum Mechanics and Thermodynamics,* 23(1), pp. 27-34.

Nollert, M. U., Panaro,, N. J. & Mcintire, L. V., 1992. Regulation of genetic expression in shear stress—stimulated endothelial cellsa. *Ann. N. Y. Acad. Sci.,* Volume 665, pp. 94-104.

Ohayon, J. et al., 2007. Influence of residual stress/strain on the biomechanical stability of vulnerable coronary plaques: Potential impact for evaluating the risk of plaque rupture. *American Journal of Physiology,* Volume 293, pp. Hl987- H1996.

Oktay, H. S., Kang, T., Humphrey, J. D. & Bishop, G. G., 1991. Changes in the mechanical behavior of arteries following balloon angioplasty. *In ASME 1991 Biomechanics Symp., AMD,* 120(New York: American Society).

Olsson, T. & Klarbring, A., 2008. Residual stresses in soft tissue as a consequence of growth and remodeling: application to an arterial geometry. *Eur. J. Mech. A/Solids,* Volume 27, pp. 959-974.

Olsson, T., Stahlhand, J. & Klarbring, A., 2006. Modeling initial strain distribution in soft tissues with application lo arteries. *Biomech. Model. Mechanobiol.,* Volume 5, pp. 28-38.

Pai, D. K., 2002. Interactive simulation of thin solids using cosserat models. *In Computer Graphics Forum,,* Volume 21, p. 347–352.

Park, H. & Lakes, R., 1986. Cosserat micromechanics of human bone: strain redistribution by a hydration sensitive constituent. *Journal of biomechanics,* 19(5), pp. 385-397.

Patel, D. J. & Fry, D. L., 1969. The elastic symmetry of arterial segments in dogs. *Circ. Res. ,* Volume 24, pp. 1-8.

Pena, E., Martinez, M. A., Calvo, B. & Doblaré, M., 2006. On the numerical treatment of initial strains in biological soft tissues. *Int. J. Numer. Methods Eng.,* Volume 68, pp. 836-860.

Pierre, B., Katia, G. & Stéphane, A., 2012. 3D residual stress field in arteries: novel inverse method based on optical full-field measurements. *Strain 40,* Volume 6, pp. 528-538.

Polzer, S. et al., 2013. A numerical implementation to predict residual strains from the homogeneous stress hypothesis with application to abdominal aortic aneurysms. *Ann. Biomed. Eng.,* 41(7), pp. 1516-1527.

Rachev, A., 1997. Theoretical study of the effect of stress-dependent remodeling on arterial geometry under hypertensive conditions. *J. Biomech.,* Volume 30, pp. 819-827.

Rachev, A. & Greenwald, S. E., 2003. Residual strains in conduit arteries. *J. Biomech,* Volume 36, pp. 661-670.

Roach, M. R. & Burton, A. C., 1957. The reason for the shape of the distensibility curve of arteries. *Can. J. Biochem.,* Volume 35, pp. 681-690.

Rock, A. D., Zhang, R. & Wilkinson, D., 2008. *Velocity varistions in cross-hole sonic logging surveys,* s.l.: Lakewood: Federal Highway Administration.

Roy, C. S., 1880-82. The elastic properties of the arterial wall. *J. Physiol,* Volume 3, pp. 125-129.

Roylance, D., 2001. *Finite Element Analysis,* s.l.: s.n.

Sack, K., 2014. *Biological tissue mechanics with fibres modelled as one dimensional Cosserat continua. Applications to cardiac tissue in healthy and diseased states,* Cape Town: The University of Cape Town.

Saini, A., Berry, C. & Greenwald, S., 1995. Effect of age and sex on residual stress in the aorta. *J. Vase. Res.,* Volume 32, pp. 398-405.

Samila, Z. J. & Carter, S. A., 1981. The effect of age on the unfolding of elastin lamellae and collagen fibers with stretch in human carotid arteries. *Can. J. Physiol. Pharm.,* Volume 59, p. 1050–1057.

Sansour, C. & Skatulla, S., 2008. A non-linear cosserat continuum-based formulation nd moving least square approximations in computations of size-scale effects in. *Computational Materials Science,* Volume 41, p. 589–601.

Sansour, C. & Skatulla, S., 2009. A strain gradient generalized continuum approach for modelling elastic scale effects. *Computer Methods in Applied Mechanics and Engineering,* 198(15-16), pp. 1401-1412.

Schröder , J. & Hoegen, M. v., 2015. *An engineering based procedure for the simulation of 3D-eigenstresses in patient-specific arteries.* s.l.:s.n.

Schröder, J. & Brinkhues, S., 2014. *A novel scheme for the approximation of residual stresses in arterial walls.* Heidelberg: Springer-Verlag.

Schulze-Bauer, C. A., Auer, M. & Holzapfel, G. A., 2002. *Layer-specific residual deformations of aged human aorta.* s.l., 13th Conference of the European Society of Biomechanics.

Schulze-Bauer, C. A. J., Morth,, C. & Holzapfel, G. A., 2003. Passive biaxial mechanical response of aged human iliac arteries. *J. Biomech. Eng.,* Volume 125, p. 395–406.

Shabana, A. A., 2012. *Computational continuum mechanics. 2nd ed.* United States of Americ: Cambridge University Press.

Shokrieh, M. M., 2014. *Residual stresses in composite materials.* First ed. Cambridge: Woodhead Publishing Limited.

Skatulla, S., Sack, K. & Sansour, C., 2015. Cosserat-fibre Continuum Approach for Myocardial Tissue. *Computational Continuum Mechanics Group.*

Skatulla, S., Sansour, C. & Hjiaj, M., 2015. On computational shells with scale effects. *Computer Methods in Applied Mechanics and Engineering,* Volume 283, pp. 46-73.

Spillmann, J. & Teschner, M., 2007. *C o r d e: Cosserat rod elements for the dynamic simulation of one-dimensional elastic objects.* s.l., Eurographics Association.

Stahlhand, J., Klarbiing, A. & Karlsson, M., 2004. Towards in vivo-aorta material identification and stress estimation. *Biomech. Model. Mechanobiol.,* Volume 2, pp. 169-186.

Takamizawa, K. & Hayashi, K., 1987. Strain energy density function and uniform strain hypothesis for arterial mechanics. *J. Biomech.,* Volume 20, pp. 7-17.

Vaishnav, R. N. & Vossoughi, J., 1983. *Estimation of residual strains in aortic segments.* In: Hall, C.W. (ed.) Biomedical Engineering II: Recent Developments. ed. New York: Pergamon Press.

Valentin, A. & Humphrey, J. D., 2009. Evaluation of fundamental hypotheses underlying constrained mixture models of arterial growth and remodelling. *Philos. Trans. R. Soc. A: Math. Phys. Eng. Sci.,* 367(1902), pp. 3585-3606.

Van Loon, P., Klip, W. & Bradley, E. L., 1977. Length-force and volume-pressure relationships of arteries. *Biorheology,* Volume 14, pp. 181-201.

Vossoughi, J., Hedjazi, Z. & Borris, F. S., 1993. Initial residual stress and strain in large;. *American Society of Mechanical Engineers,* Issue In: Langrnna, N./\., Friedman. M.H. , Groml, E.S. (eds.) Proceedings of the Summer Bioengineeiing Conference, pp. 434-437.

Wan, L. Q., Guo, X. E. & Mow, V. C., 2010. A triphasic orthotropic laminate model for cartilage curling behaviour: fixed charge density vs. mechanical properties. *J. Biomceb. Eng.,* Volume 132, p. 024504.

Weber, K. T., 1989. Cardiac interstitium in health and disease: the fibrillar collagen network. *Journal of the American College of Cardiology,* 13(7), pp. 1637-1652.

Weizsacker, H. W., Lambert, H. & Pascale, K., 1983. Analysis of the passive mechanical properties of rat carotid arteries. *J. Biomech.,* Volume 16, pp. 703-715.

Weizsacker, H. W. & Pinto, J. C., 1988. Isotropy and anisotropy of the arterial wall. *J. Biomech,* Volume 21, pp. 477-487.

Wolinsky, H. & Glagov, S., 1969. Comparision of abdominal and thoracic aortic media structure in mammals. *Circ. Res. ,* Volume 25, pp. 677-686.

Zeller, p. j. & Skalak, T. C., 1998. Contribution of individual structural components in determining the zero-stress state in small. *J. Vase. Res.,* Volume 35, pp. 8-17.